

**WP1 – NUMERICAL BENCHMARK INVESTIGATION**

# Table of contents

1	Introduction.....	3
2	1 <sup>st</sup> example: beam under pure bending .....	3
2.1	Definition of load application and boundary conditions.....	4
2.2	Definition of the geometry and mesh.....	5
2.3	Results.....	6
3	2 <sup>nd</sup> example: Constant cross-section beam subjected to lateral torsional buckling.....	7
3.1	Definition of load application and boundary conditions.....	8
3.2	Definition of the geometry and mesh.....	8
3.3	Results.....	9
4	3 <sup>rd</sup> example: tapered beam subjected to lateral torsional buckling .....	11
4.1	Definition of load application and boundary conditions.....	12
4.2	Definition of the geometry and mesh.....	12
4.3	Results.....	13
5	4 <sup>th</sup> example: columns under axial compression and eccentric load .....	15
5.1	Definition of load application and boundary conditions.....	15
5.2	Definition of the geometry and mesh.....	17
5.3	Results.....	17
6	5 <sup>th</sup> example: columns under axial compression and eccentric load .....	20
6.1	Definition of load application and boundary conditions.....	20
6.2	Definition of the geometry and mesh.....	21
6.3	Results.....	22
7	6 <sup>th</sup> example: single span frame.....	25
7.1	Definition of load application and boundary conditions.....	25
7.2	Definition of the geometry and mesh.....	27
7.3	Results.....	27
8	Conclusion .....	29

# 1 Introduction

In order to develop various numerical parametric studies for fire resistance assessment of steel structures with welded or hot-rolled class 4 steel members with three different computer codes (ABAQUS, ANSYS and SAFIR), it is necessary to ensure the result consistency among these different codes and among the assumptions chosen by each partner of the project. With this aim, a numerical benchmark investigation is carried out, in which all important parameters are settled for the parametric study of the project.

In this section are simply described all the examples that are developed by the modelling group of the project in order to ensure that the numerical simulations carried out with different computer codes have the same input parameters which should lead to similar results in terms of failure load or critical temperature. Steel S355 based on EN 1993-1-2 definition is used in all examples. Regarding to the shell elements to be used, the 1<sup>st</sup> order shell elements are proposed. These shells have four nodes and six degrees of freedom at each of these nodes (three translational degrees of freedom and three rotational degrees of freedom).

## 2 1<sup>st</sup> example: beam under pure bending

For the first example, the investigated beam is a constant cross-section. Web and flanges are class 4 and are consequently sensitive to local buckling. The beam is subjected to 4-point bending and stiffeners are present at both load points and supports. Lateral restraints are applied at the stiffeners locations. The beam is heated at a stabilized temperature of 450 °C in its middle 1.5 m length. The following picture illustrates these conditions and dimensions:

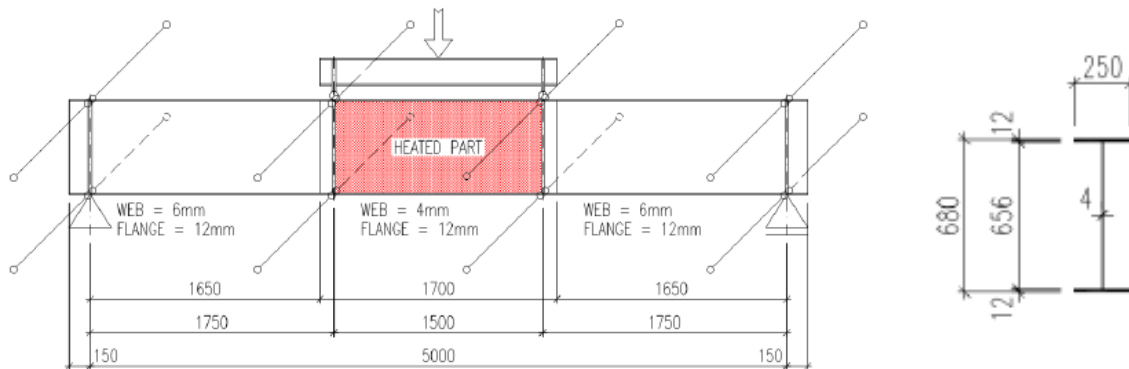


Figure 1 : Beam subjected to pure bending

## 2.1 Definition of load application and boundary conditions

In order to ensure that the numerical simulations carried out with the three different computer codes lead to similar results, the same boundary conditions are adopted by the modelling group. In this first example, the boundary conditions proposed by partner 5 are used for the development of these models. At the supports and at the points where load is applied, the whole cross-section is transversally restrained. One of the supports allows free horizontal displacement (see Figure 2). Only the internal span is considered to be heated up, while the rest of the beam and stiffeners are considered to be at room temperature:

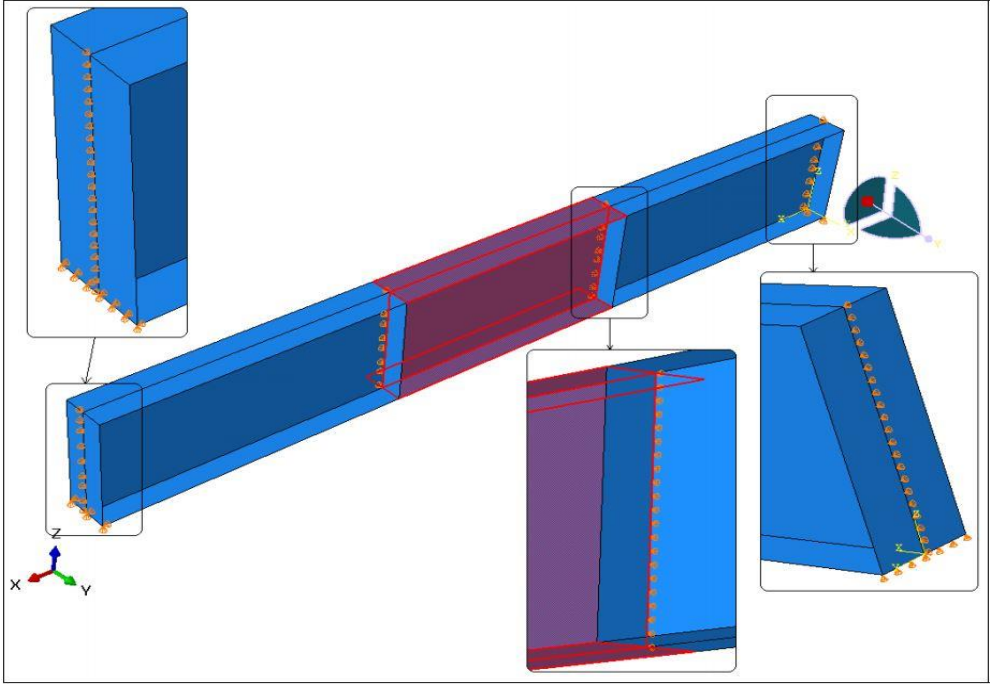


Figure 2: Boundary conditions and illustration of the heated part

Loads are applied on the upper flange to all nodes drawing the line of the defined load application zone, see following figure:

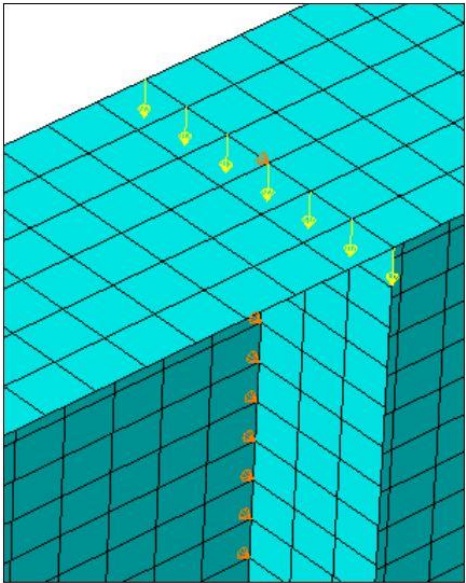


Figure 3: Load application on the upper flange

## 2.2 Definition of the geometry and mesh

In order to avoid any undesirable effects at the load application nodes, end plates and stiffeners with a thickness of 20 mm are modelled in the numerical simulations.

As the linear buckling analysis is not available in computer code SAFIR, imperfections are introduced considering a sinusoidal deformed mesh, whereas in ABAQUS and ANSYS, imperfections can be defined as a linear superposition of buckling Eigen-modes. Moreover, from some previous numerical simulations carried out by the modelling group of the project when defining the test set up, it has been observed that the global imperfection has the major influence in the load bearing capacity of the studied beam. Therefore, and to reduce the possible input differences among the three computer codes, only the use of a global imperfection with an amplitude  $L/300$ , with L the distance between lateral supports ( $L=1.5$  m), was introduced. Thus, the global imperfection is 5 mm. The following figure illustrates the shape of this global imperfection:

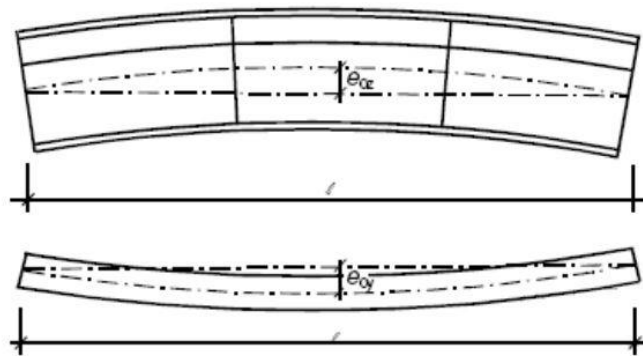


Figure 4: Shape of the global imperfection

For a harmonized numerical simulation, the following mesh size is proposed to all the partners. The number of elements in which each side is divided is represented in the figure below:

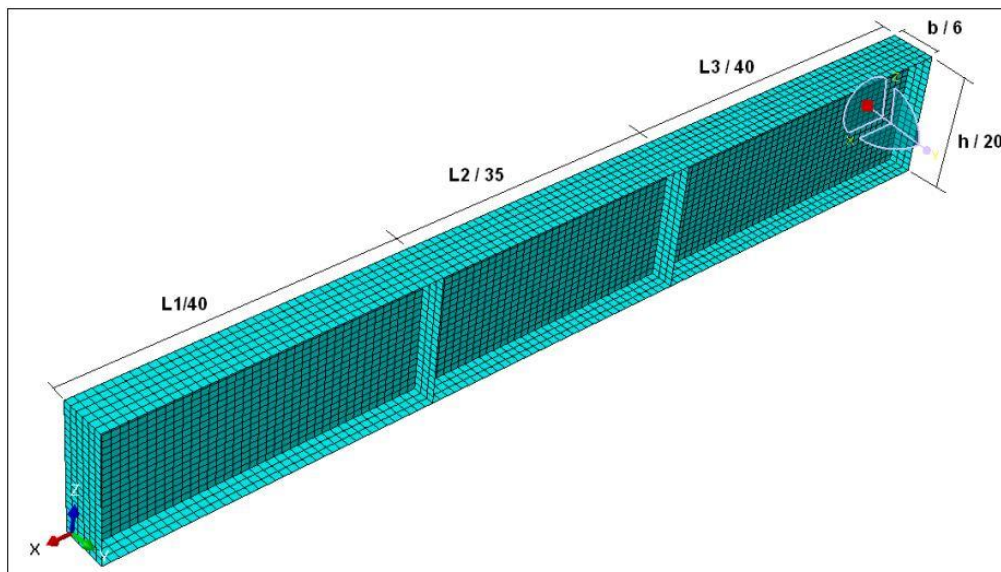


Figure 5: Definition of the mesh size

## 2.3 Results

The tables and figures below illustrate the failure load, ultimate bending moment and load deflection curve obtained by all partners for the 1<sup>st</sup> example of the benchmark study under the three different computer codes:

FAILURE LOAD (kN)				
CTICM (ANSYS)	CTU (ABAQUS)	TECNALIA (ABAQUS)	UAVR (SAFIR)	ULG (SAFIR)
306.19	284.98	307.03	284.22	286.91
ULTIMATE BENDING MOMENT (kN.m)				
CTICM (ANSYS)	CTU (ABAQUS)	TECNALIA (ABAQUS)	UAVR (SAFIR)	ULG (SAFIR)
535.84	498.72	537.30	497.38	502.10

Table 1: Failure load and ultimate bending moment for the 1<sup>st</sup> example

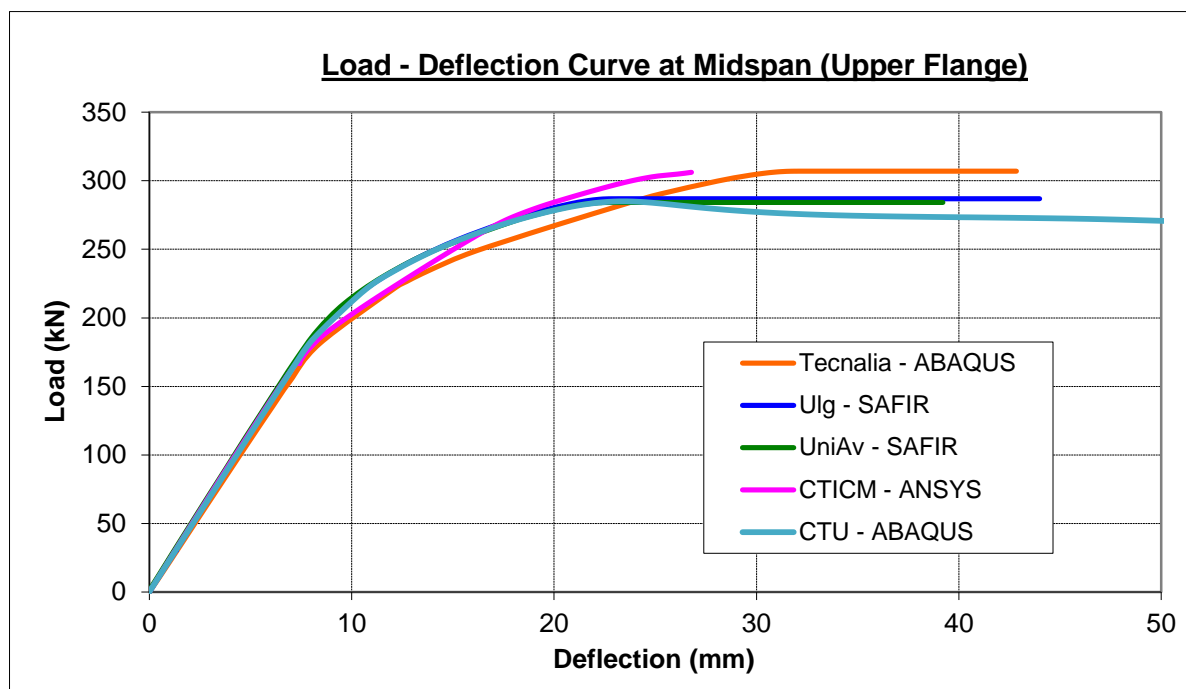
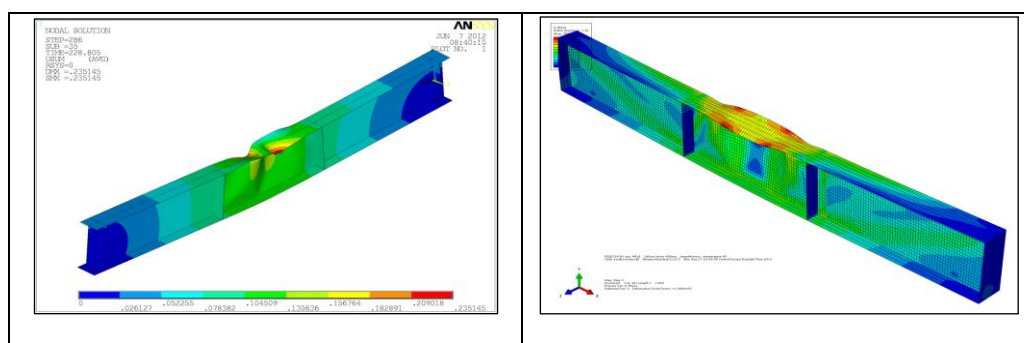
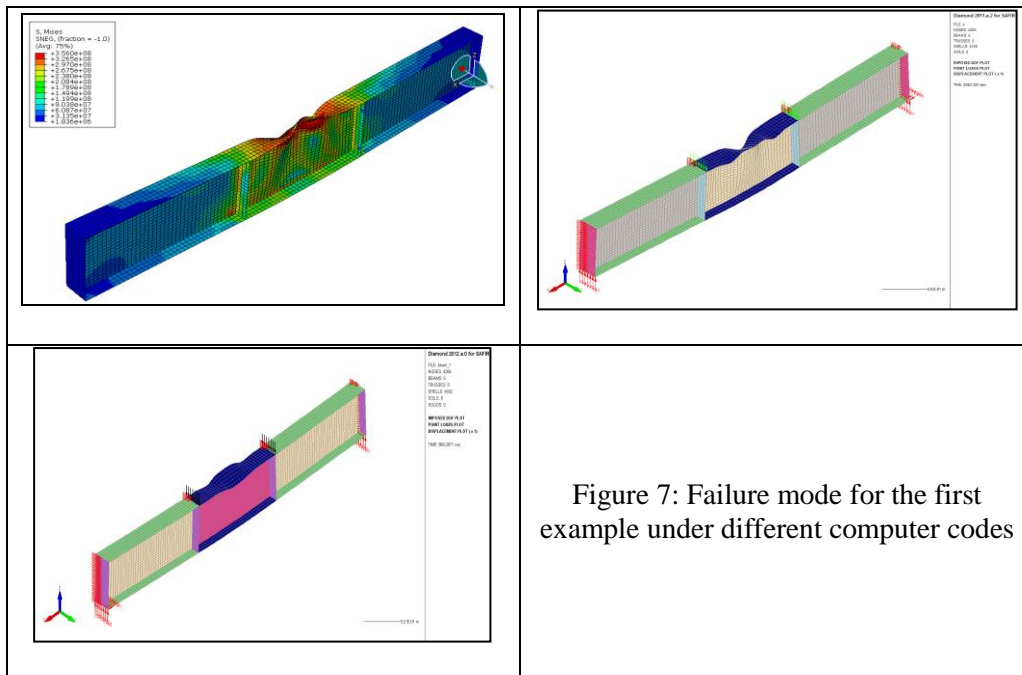


Figure 6: Load-deflection curve at mid-span (upper flange) for the 1<sup>st</sup> example

The failure modes of the beam obtained with the different softwares are shown hereafter:





### 3 2<sup>nd</sup> example: Constant cross-section beam subjected to lateral torsional buckling

The beam with constant cross-section shown in the figure below consists of a class 4 web and of class 4 flanges. The beam is subjected to 4-point bending, with stiffeners at both load points and supports. Lateral restraints are applied at the four stiffeners location. The beam is loaded at a stabilized temperature of 450 °C, which is constant over the middle 2.8 m length, as shown in the following figure:

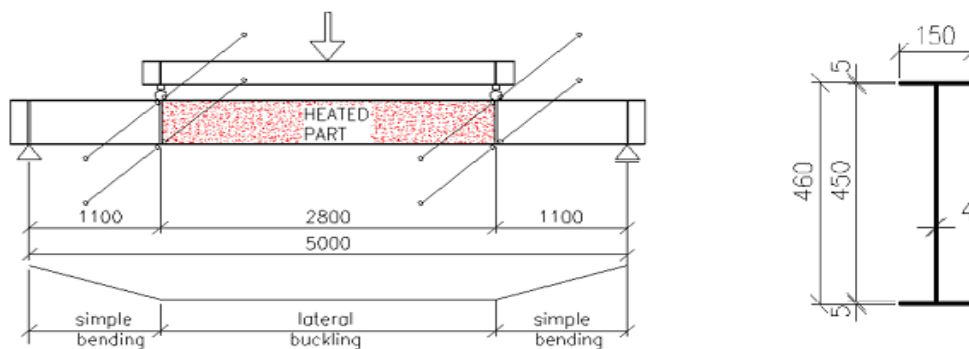


Figure 8: 2<sup>nd</sup> example for benchmark study

### 3.1 Definition of load application and boundary conditions

The boundary conditions proposed for the second example are represented in Figure 9. At the locations of the applied loads, the whole cross-section is transversally restrained. The supports are considered only by one node. The first node prevents displacements in all directions, while the other one allows free horizontal displacement. Rotations in all directions are free for both supports. Only the internal span is considered to be heated up, while the rest of the beam and stiffeners are considered to be at room temperature:

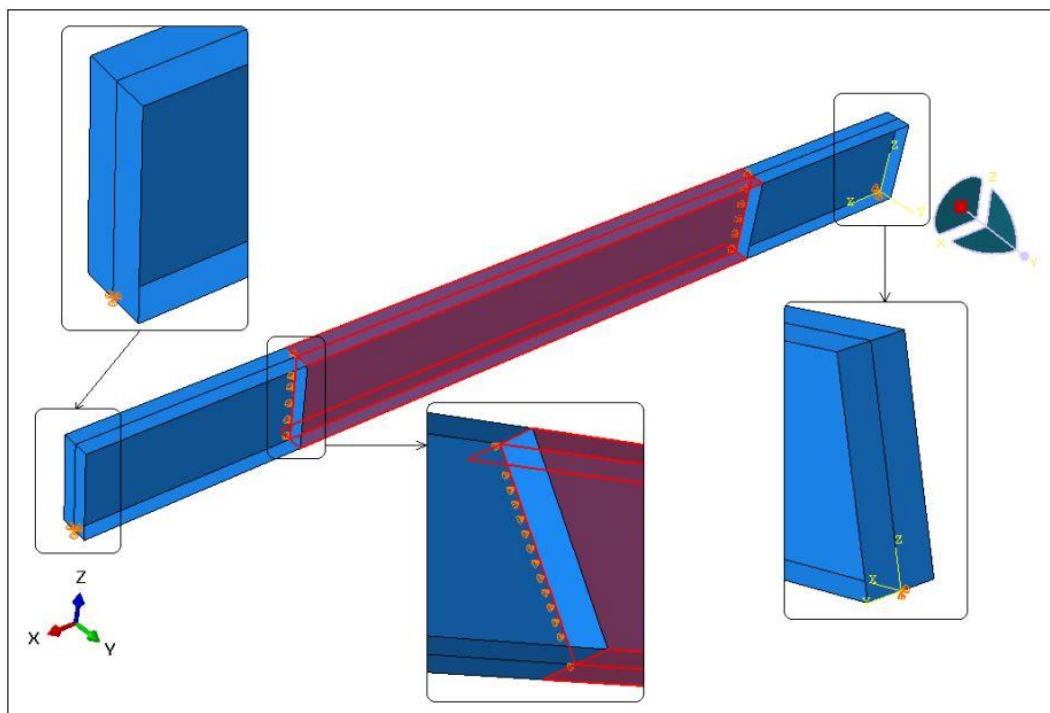


Figure 9: Boundary conditions and illustration of the heated part

Loads are applied on the upper flange to all nodes drawing the line of the defined load application zone, as for the first example, see Figure 3.

### 3.2 Definition of the geometry and mesh

In order to avoid any undesirable effects at the load application nodes, stiffeners with a thickness of 20 mm are modelled in the numerical simulations whereas end plates have a thickness of 10 mm.

Following the same assumption as for the first example, only the use of a global imperfection is made. The amplitude is proposed as:  $L/1000$ .  $L$  is the distance between lateral supports, which is equal to 2.8 m. Thus, the global imperfection is 2.8 mm. Figure 4 illustrates the shape of this global imperfection

For a harmonized numerical simulation, the following mesh size is proposed to all partners. The number of elements in which each side is divided is represented in the figure below:

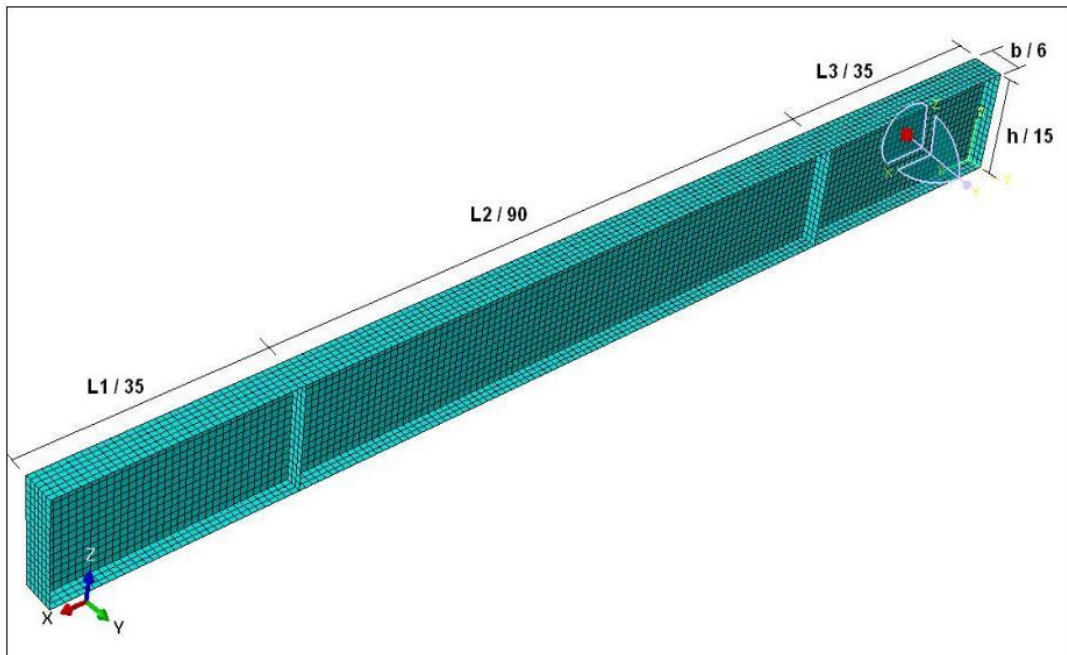


Figure 10: Definition of mesh size

### 3.3 Results

The tables and figures below illustrate the failure load, ultimate bending moment and load deflection curve obtained by all partners for the 2<sup>nd</sup> example of the benchmark study under the three different computer codes:

FAILURE LOAD (kN)				
CTICM (ANSYS)	CTU (ABAQUS)	TECNALIA (ABAQUS)	UAVR (SAFIR)	ULG (SAFIR)
56.10	52.11	55.10	52.07	61.16
ULTIMATE BENDING MOMENT (kN.m)				
CTICM (ANSYS)	CTU (ABAQUS)	TECNALIA (ABAQUS)	UAVR (SAFIR)	ULG (SAFIR)
61.70	57.32	60.61	57.28	67.28

Table 2: Failure load and ultimate bending moment for the 2<sup>nd</sup> example

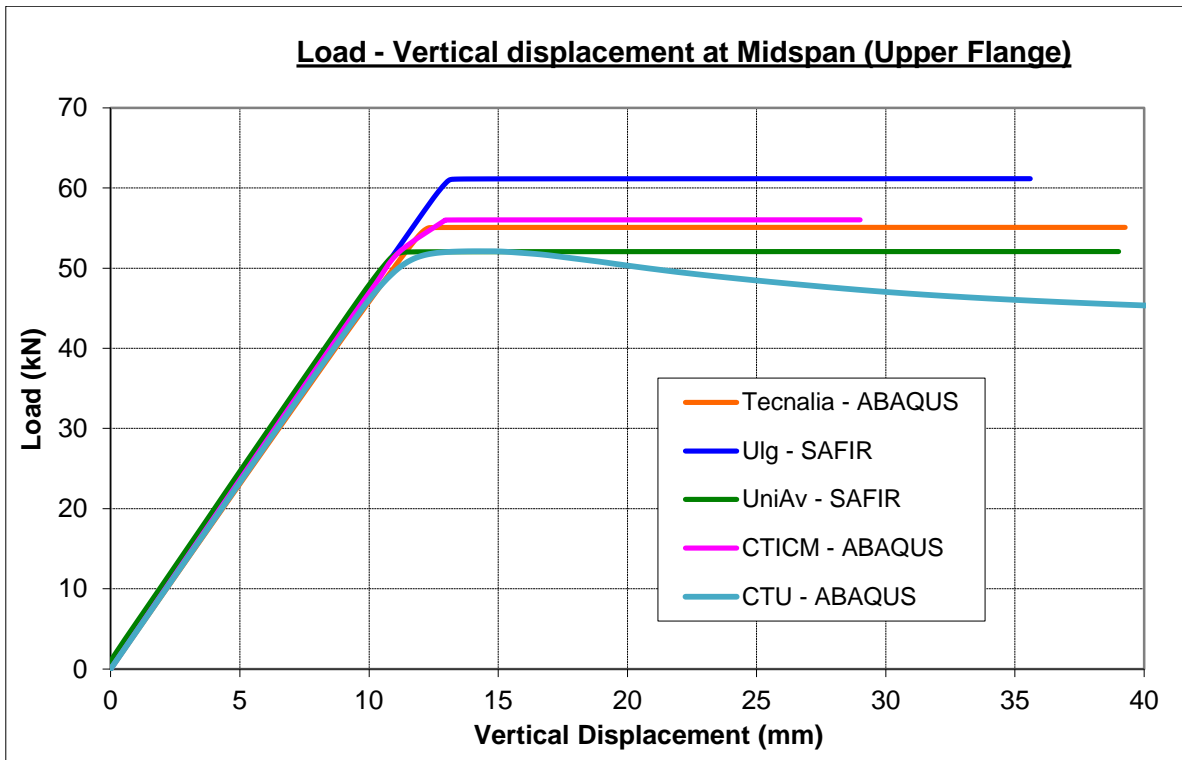
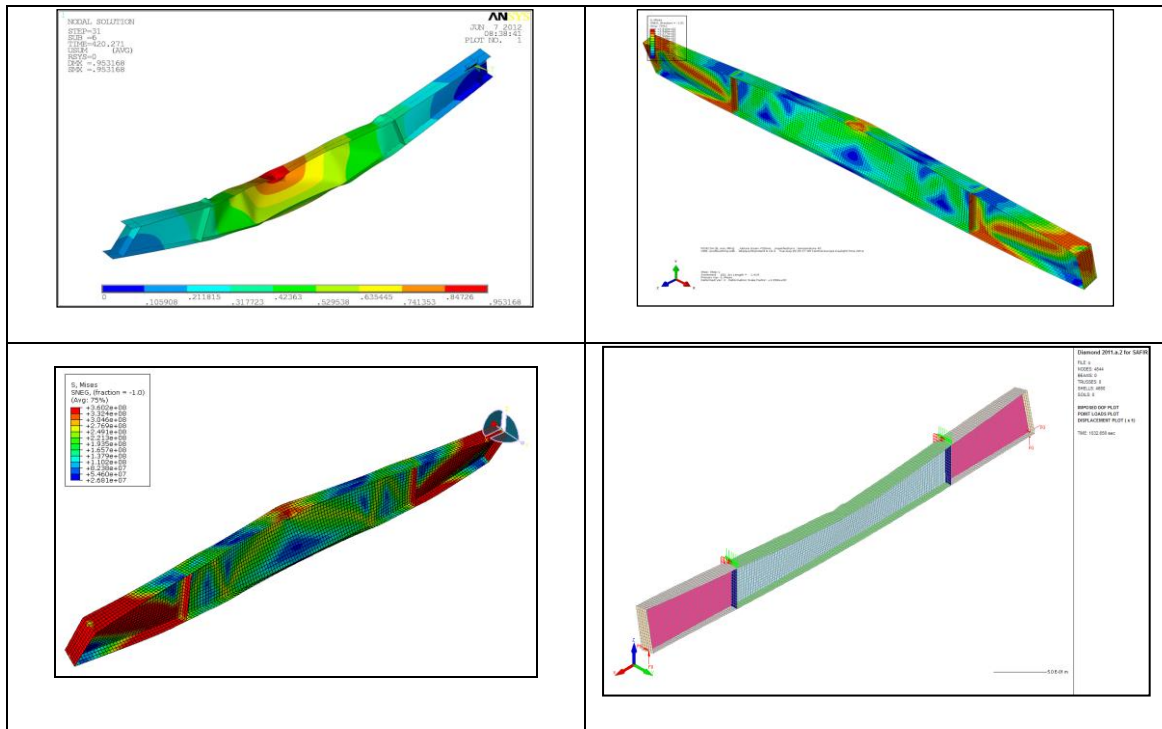
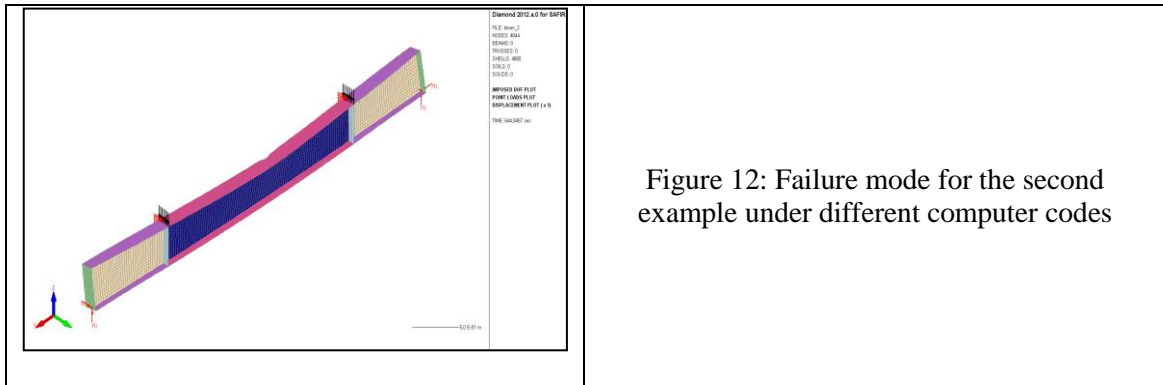


Figure 11: Load-deflection curve at mid-span (upper flange) for the 2<sup>nd</sup> example

The failure modes of the beams of example 2 obtained with the different softwares are shown hereafter:





### 4 3<sup>rd</sup> example: tapered beam subjected to lateral torsional buckling

The beam shown in the figure below consists of a variable cross-section. The beam is subjected to 4-point bending, with stiffeners at both load points and supports. Lateral restraints are applied at the four stiffeners location. The beam is loaded at a stabilized temperature of 650 °C, which is uniform over the middle 2.8 m length, as shown in Figure 13:

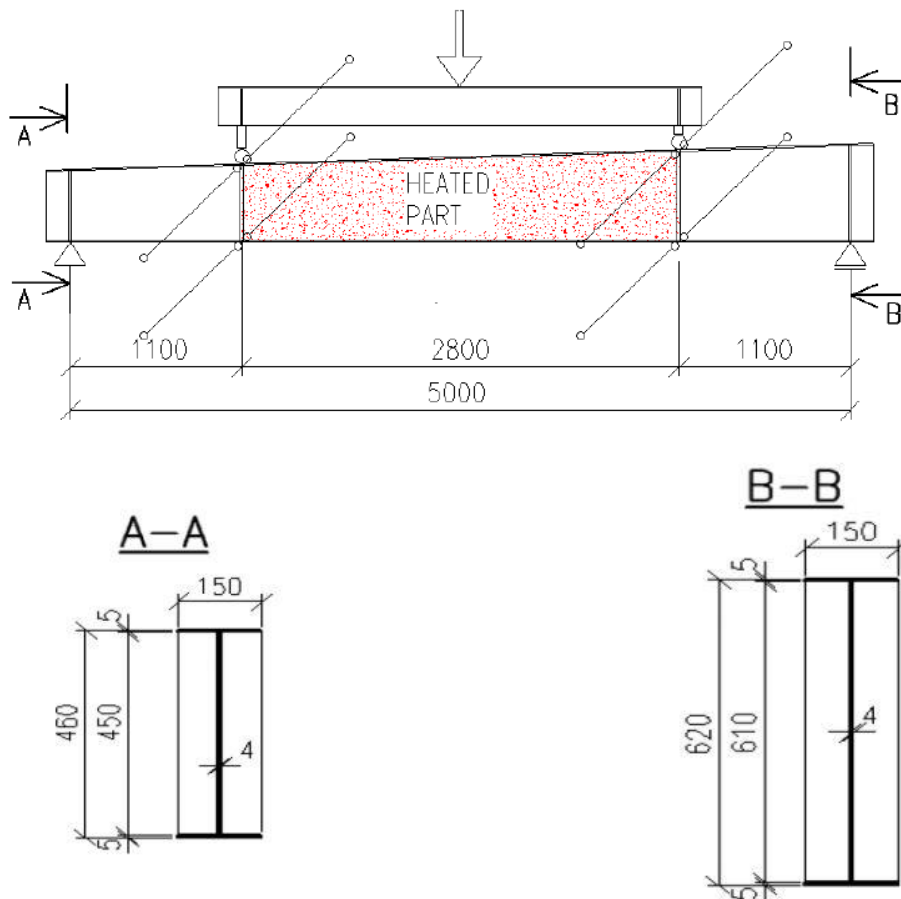


Figure 13: 3<sup>rd</sup> example for benchmark study

## 4.1 Definition of load application and boundary conditions

The boundary conditions proposed for the third example are represented in Figure 14. At the locations of the applied loads, the whole cross-section is transversally restrained. The supports are considered only by one node. The first node prevents displacements in all directions, while the other one allows free horizontal displacement. Rotations in all directions are free for both supports. Only the internal span is considered to be heated up, while the rest of the beam and stiffeners are considered to be at room temperature:

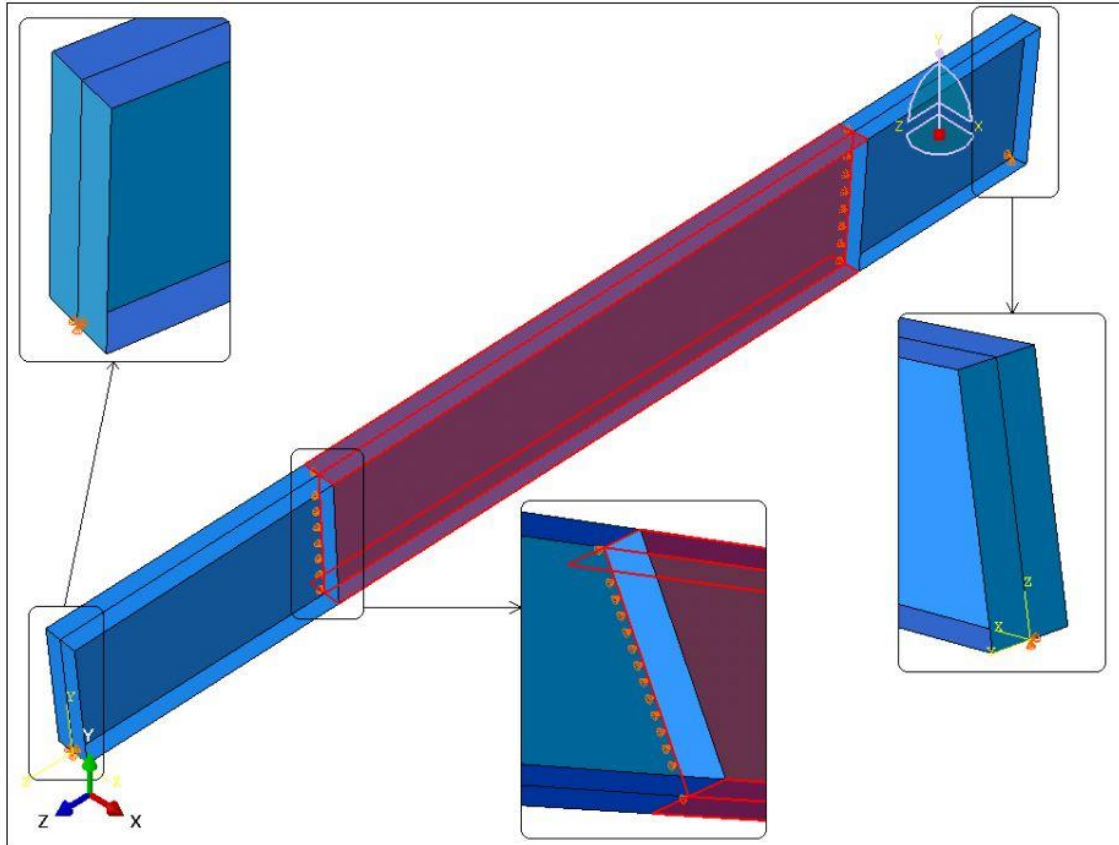


Figure 14: Boundary conditions and illustration of the heated part

Loads are applied on the upper flange to all nodes drawing the line of the defined load application zone, as for the first example, see Figure 3.

## 4.2 Definition of the geometry and mesh

In order to avoid any undesirable effects at the load application nodes, stiffeners with a thickness of 20 mm are modelled in the numerical simulations whereas end plates have a thickness of 10 mm.

Following the same assumption as for the first example, only the use of a global imperfection is made. The amplitude is proposed as  $L/1000$ .  $L$  is the distance between lateral supports, which is equal to 2.8 m. Thus, the global imperfection is 2.8 mm. Figure 4 illustrates the shape of this global imperfection.

For a harmonized numerical simulation, the following mesh size is proposed to all partners. The number of elements in which each side is divided is represented in the figure below:

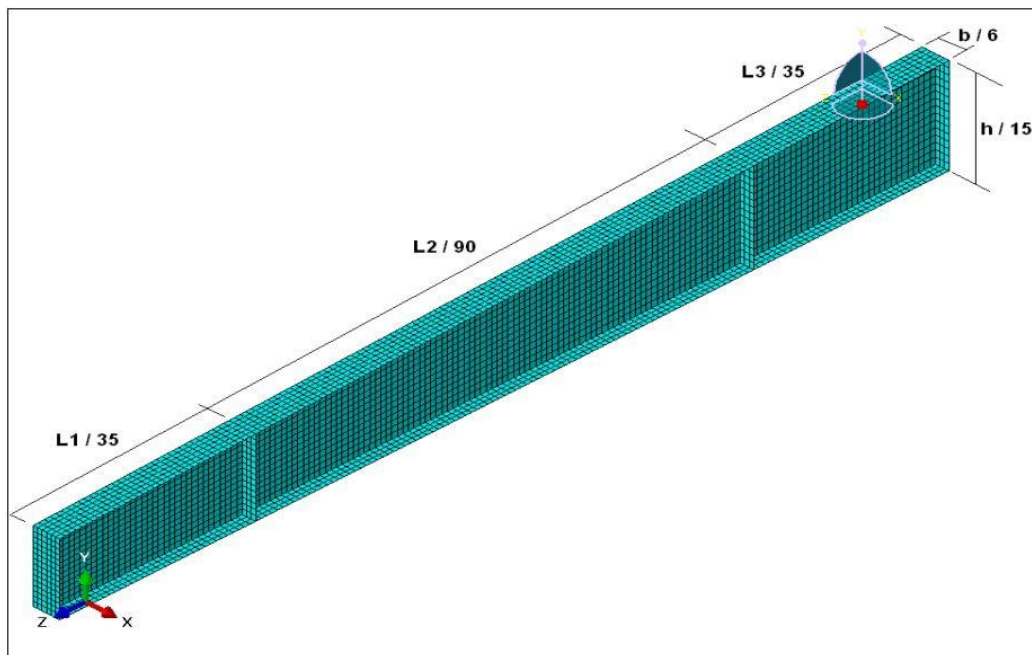


Figure 15: Definition of mesh size

### 4.3 Results

The tables and figures below illustrate the failure load, ultimate bending moment and load deflection curve obtained by all partners for the 3<sup>rd</sup> example of the benchmark study under the three different computer codes:

FAILURE LOAD (kN)			
CTICM (ANSYS)	CTU (ABAQUS)	TECNALIA (ABAQUS)	ULG (SAFIR)
30.13	29.89	29.19	31.19
ULTIMATE BENDING MOMENT (kN.m)			
CTICM (ANSYS)	CTU (ABAQUS)	TECNALIA (ABAQUS)	ULG (SAFIR)
33.14	32.88	32.11	34.31

Table 3: Failure load and ultimate bending moment for the 3<sup>rd</sup> example

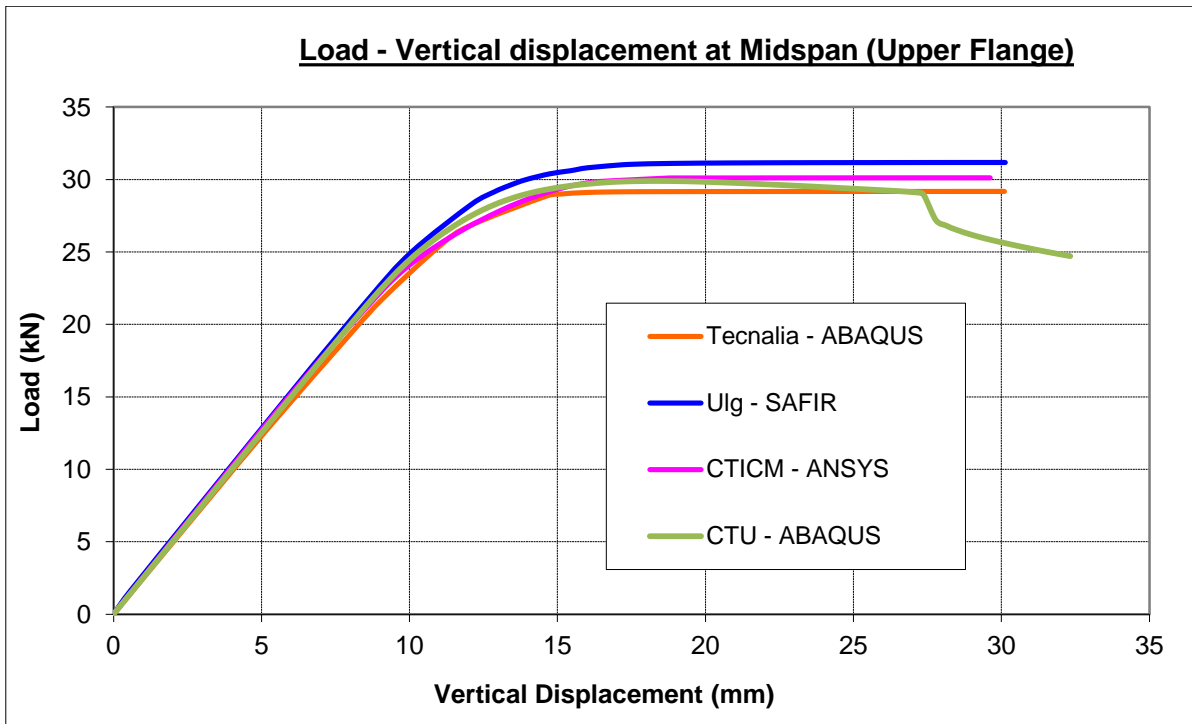
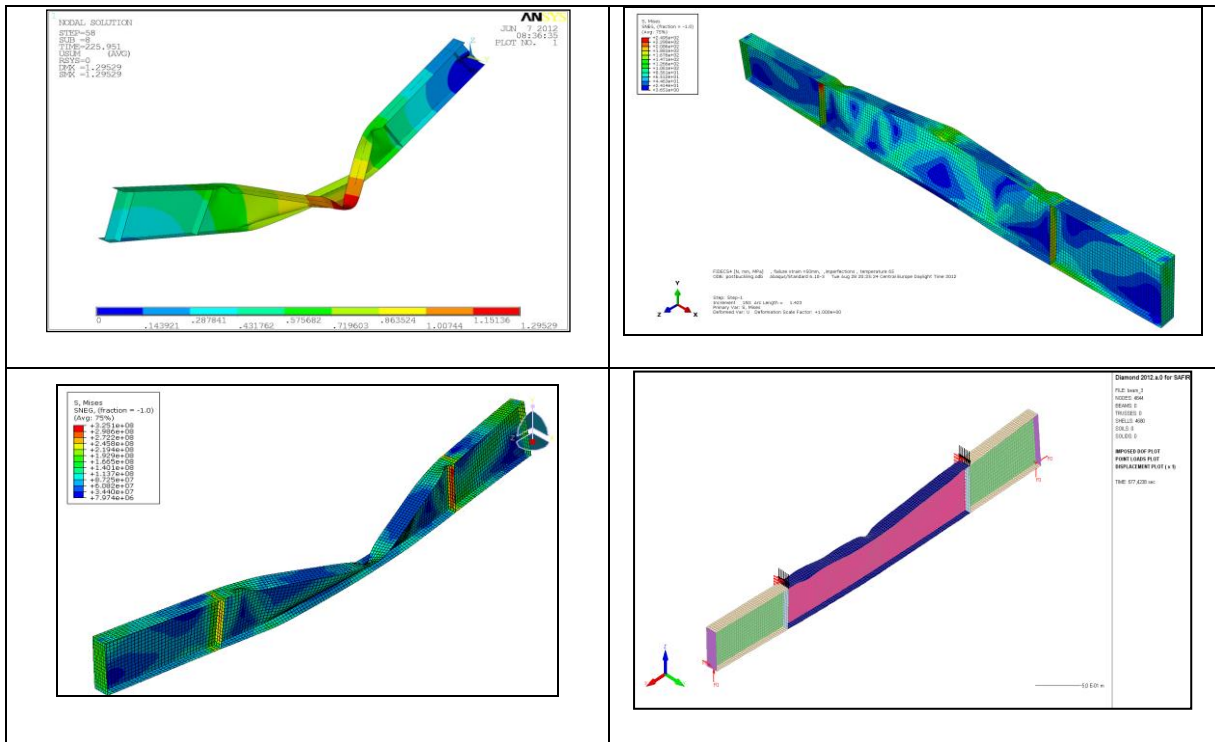


Figure 16: Load-deflection curve at mid-span (upper flange) for the 3<sup>rd</sup> example

The failure modes of the beams of example 3 obtained with the different softwares are shown hereafter:



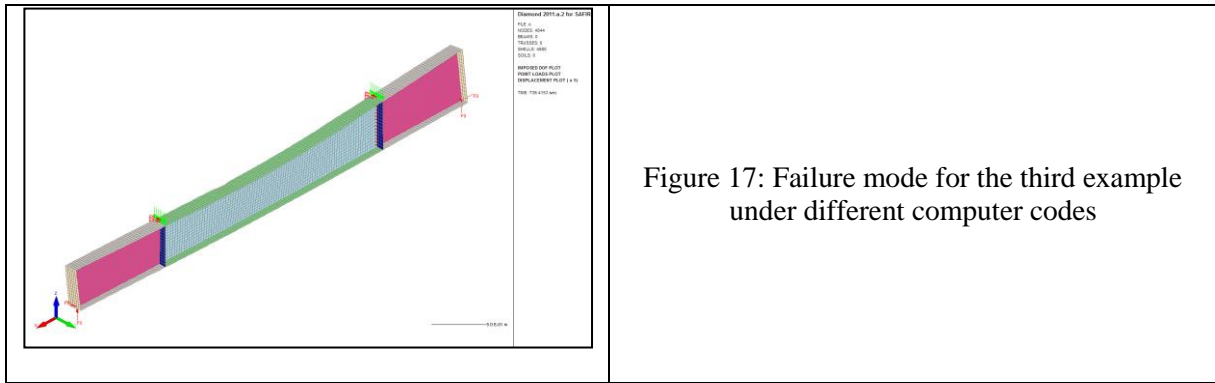


Figure 17: Failure mode for the third example under different computer codes

## 5 4<sup>th</sup> example: columns under axial compression and eccentric load

The column with constant cross-section shown in the figure consists on a class 4 web and class 4 flanges. An eccentric axial load about the major axis is applied on the column. It is heated along its whole length, after reaching a mechanical load ratio:

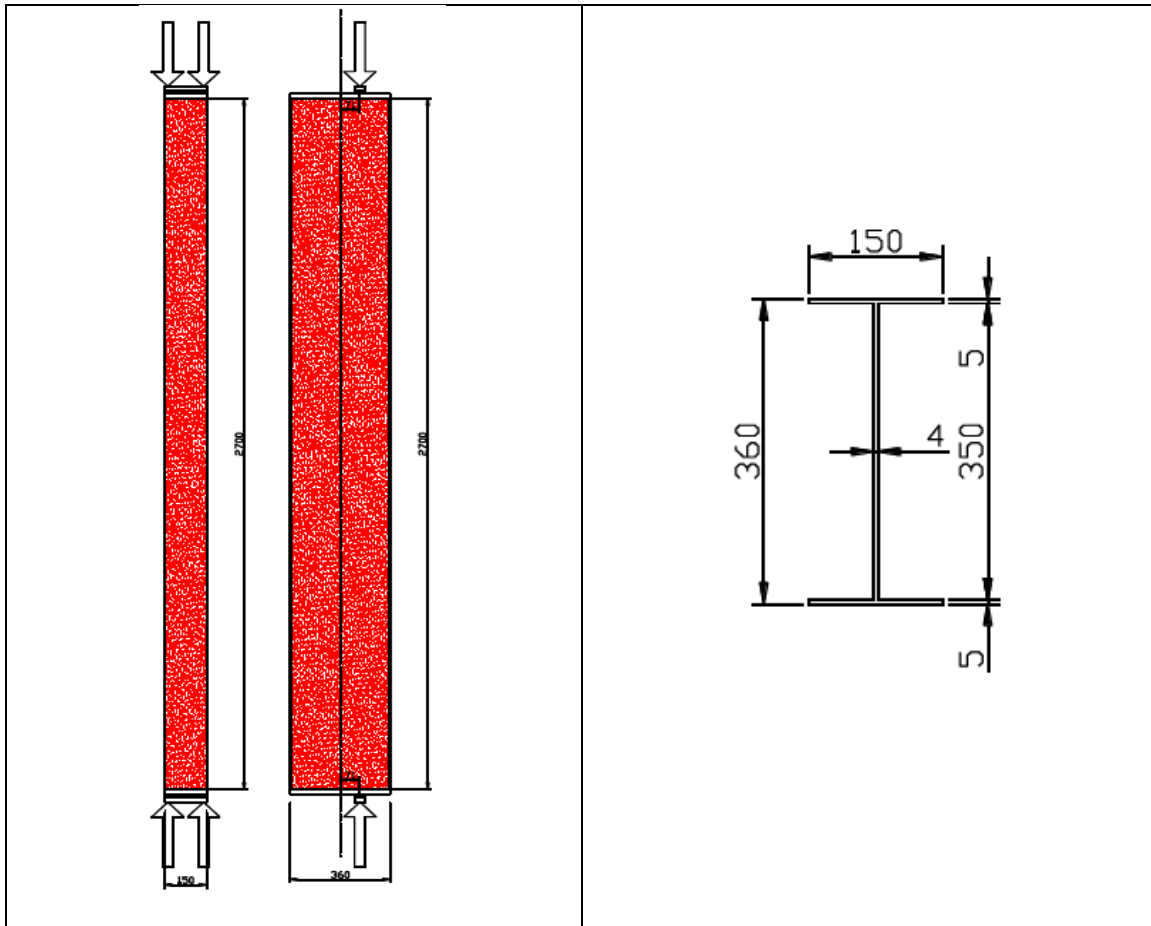


Figure 18: 4<sup>th</sup> example for benchmark study

### 5.1 Definition of load application and boundary conditions

The boundary conditions proposed for the fourth example are represented in Figure 19. In this example, the boundary conditions proposed by partner 5 are used for the development of these models. At both supports, deformation and rotation in z-z direction are restrained. Rotation about x-x axis is also

restrained. Only one node is blocked in the direction of the y-y axis. At the bottom support, in addition, nodes are also blocked in the vertical direction (x-x). The column is heated up in all its length, including the end plates:

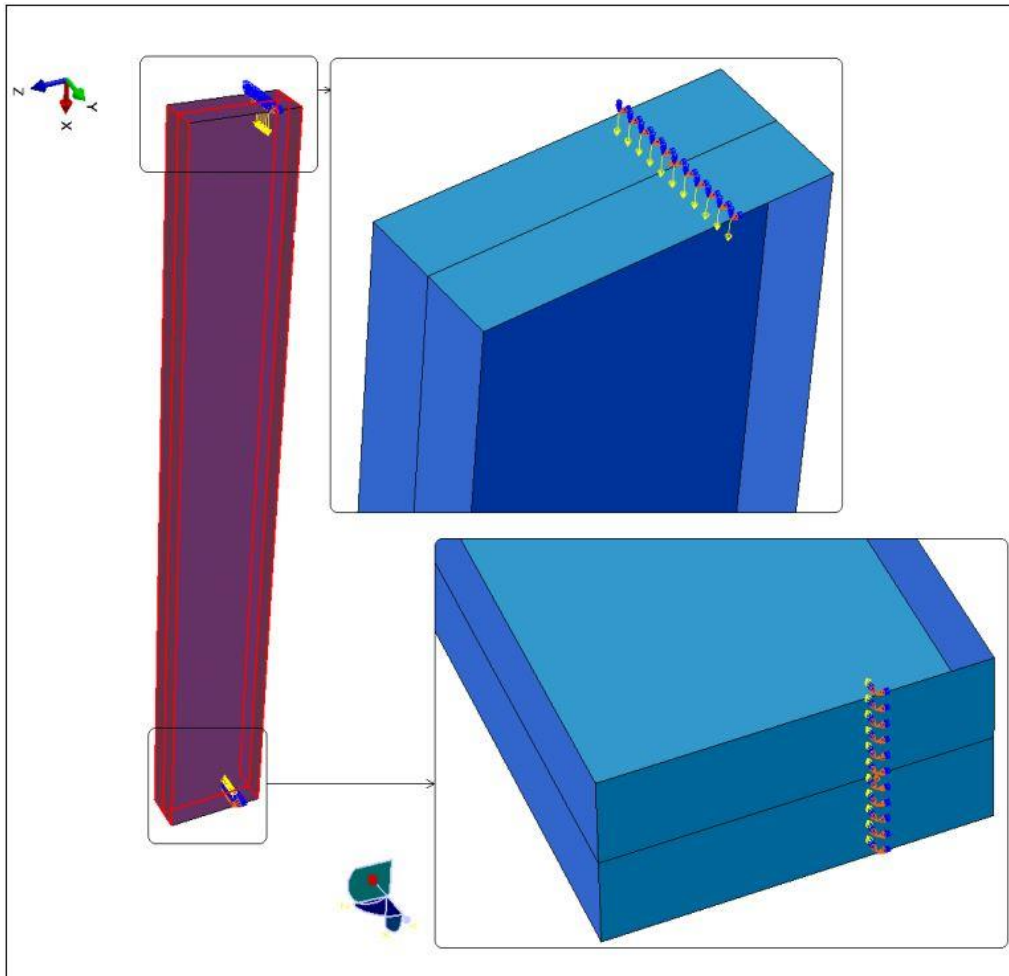


Figure 19: Boundary conditions and illustration of the heated part

On the superior end plate, the load is applied to all the nodes drawing the line of the load application zone:

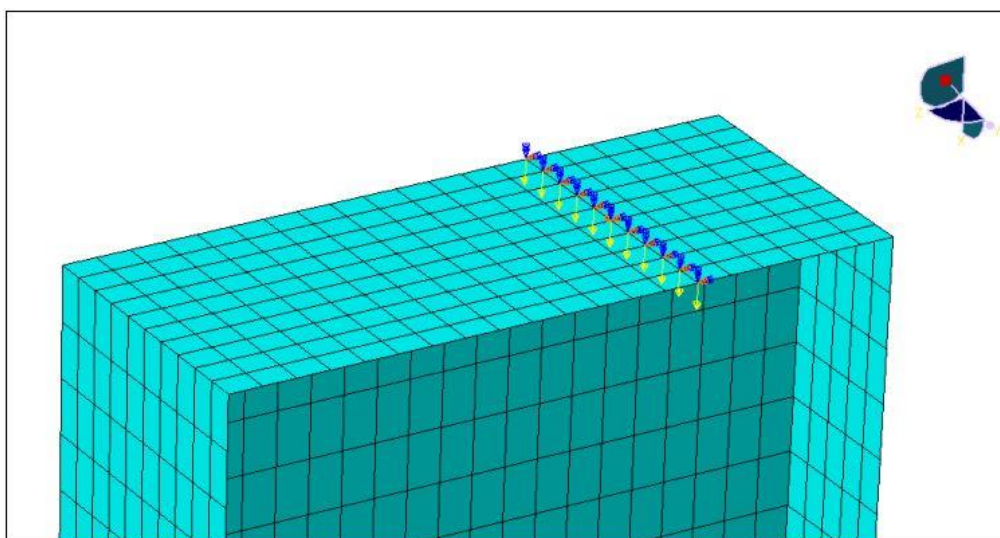


Figure 20: Load application on the upper end plate

## 5.2 Definition of the geometry and mesh

In order to avoid any undesirable effects in the load application points, a thickness of 30 mm will be adopted for both end plates.

Following the same assumption as for the first example, only the use of a global imperfection is made. The amplitude is proposed as:  $L/500$ .  $L$  is the distance between both end plates, which is equal to 2.7 m. Thus, the global imperfection is 5.4 mm. Figure 4 illustrates the shape of this global imperfection.

For a harmonized numerical simulation, the following mesh size is proposed to all partners. The number of elements in which each side is divided is represented in the figure below:

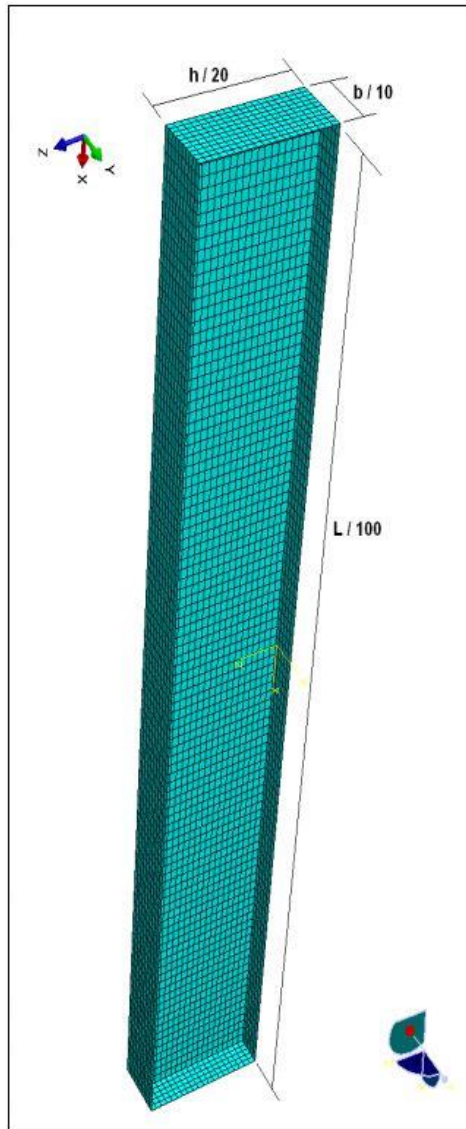


Figure 21: Definition of mesh size

## 5.3 Results

The following tables and figures illustrate the failure load and load horizontal displacement in the strong axis obtained by the partners for the 4<sup>th</sup> example of the benchmark study under the three different computer codes:

FAILURE LOAD (kN) at 500 °C				
CTICM (ANSYS)	CTU (ABAQUS)	TECNALIA (ABAQUS)	UAVR (SAFIR)	ULG (SAFIR)
235.50	232.71	221.98	207.70	226.56

Figure 22: Failure load of column from the 4<sup>th</sup> example

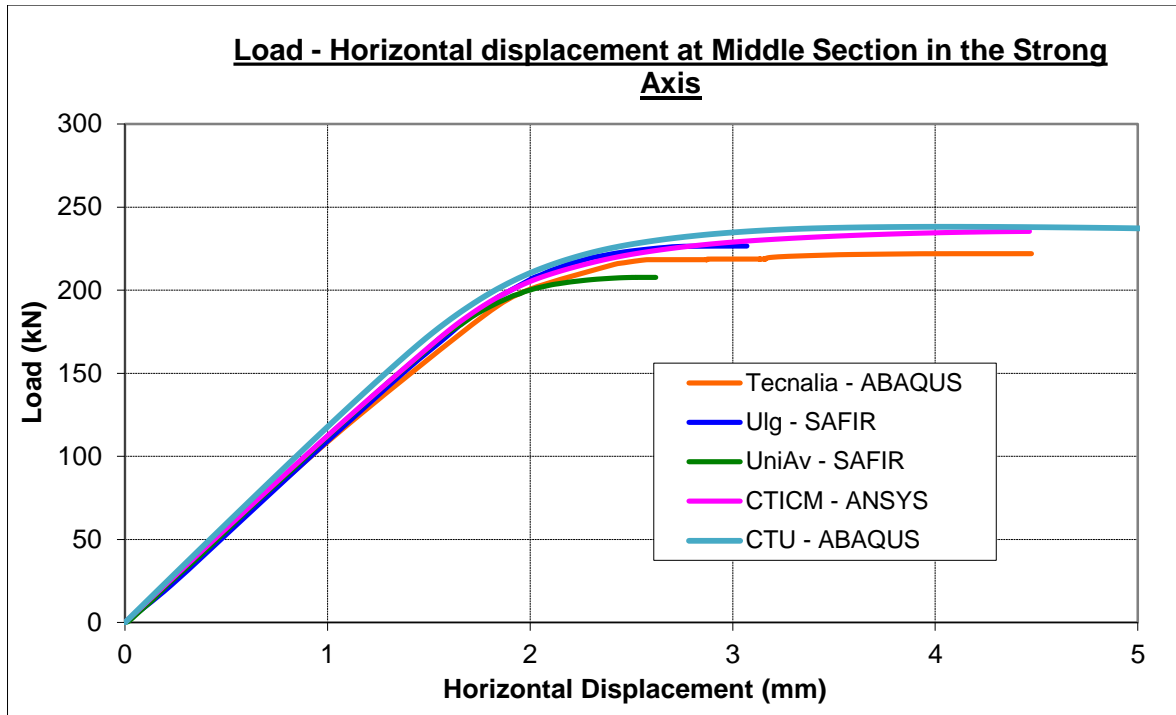
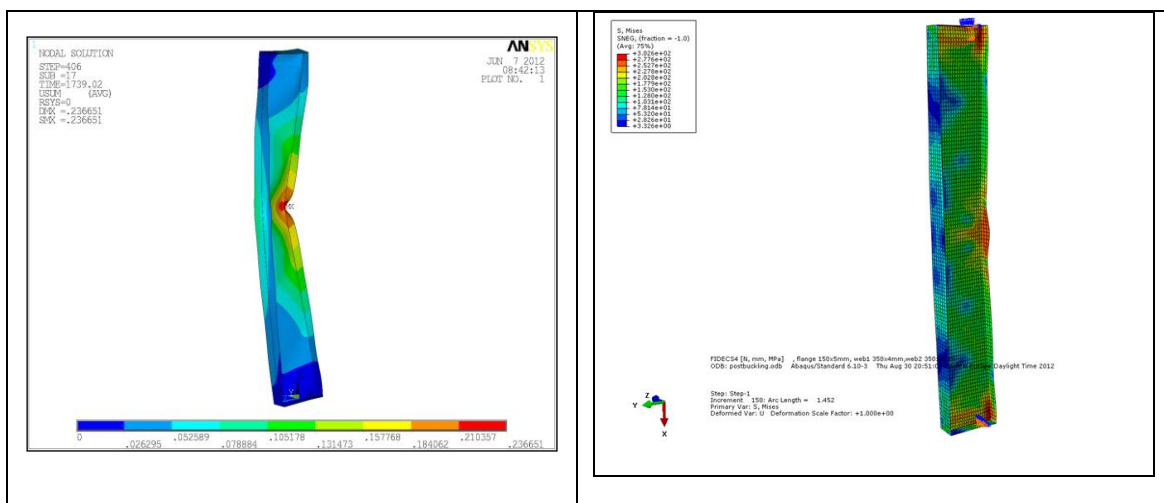


Figure 23: Load – horizontal displacement at middle section in the strong axis for the 4<sup>th</sup> example

The failure modes of the beams of example 4 obtained with the different softwares are shown hereafter:



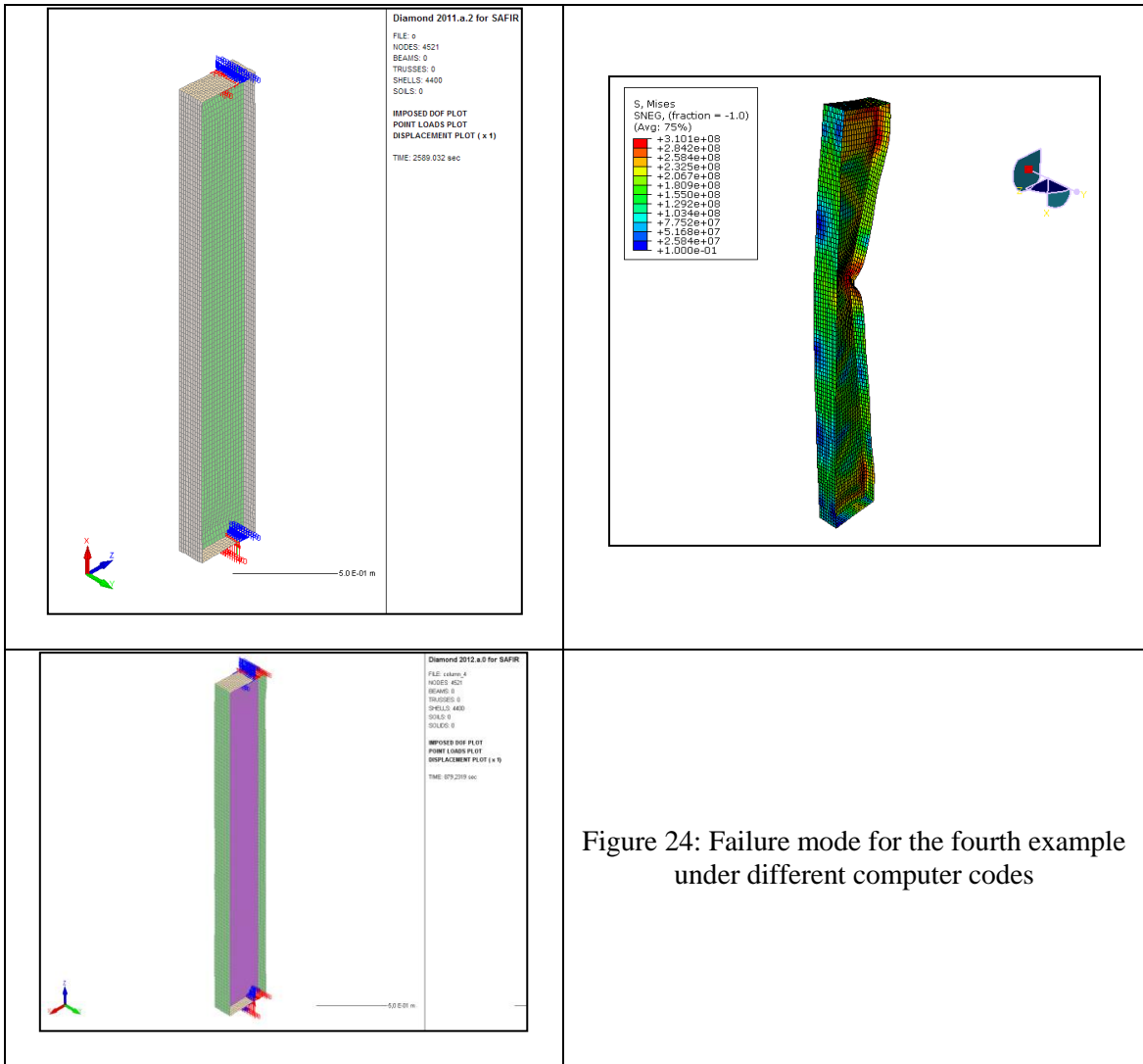


Figure 24: Failure mode for the fourth example under different computer codes

## 6 5<sup>th</sup> example: columns under axial compression and eccentric load

The column with variable cross-section shown in the figure consists of a class 4 web and of class 4 flanges. An eccentric axial load along the column's major axis is applied. The column is heated along its whole length, after reaching a mechanical load ratio:

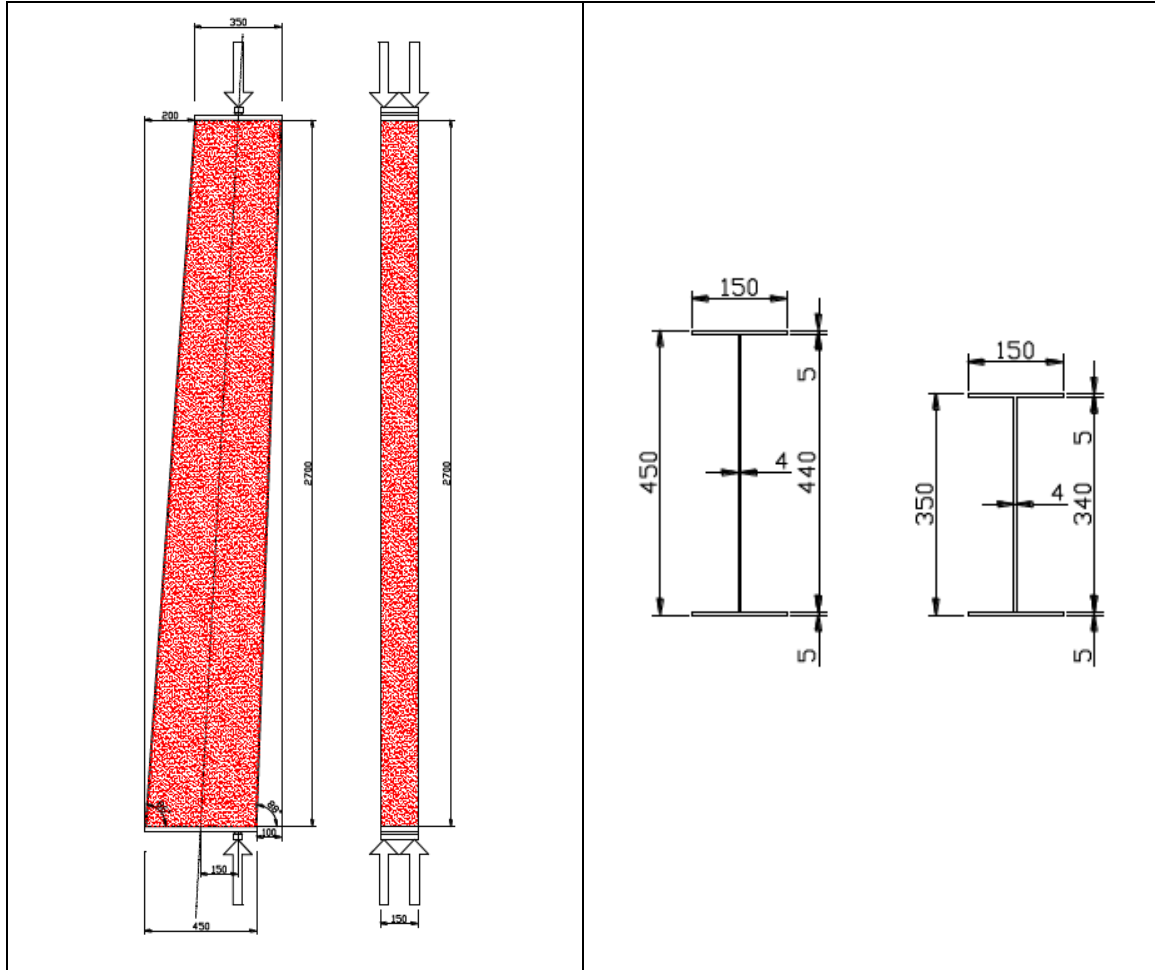


Figure 25: 5th example for benchmark study

### 6.1 Definition of load application and boundary conditions

The boundary conditions proposed for the fourth example are represented in Figure 26. In this example, the boundary conditions proposed by partner 5 are used for the development of these models. At both supports, deformation and rotation in z-z direction are restrained. Rotation about x-x axis is also restrained. Only one node is blocked in the direction of the y-y axis. At the bottom support, in addition, nodes are also blocked in the vertical direction (x-x). The column is heated up in all its length, including the end plates:

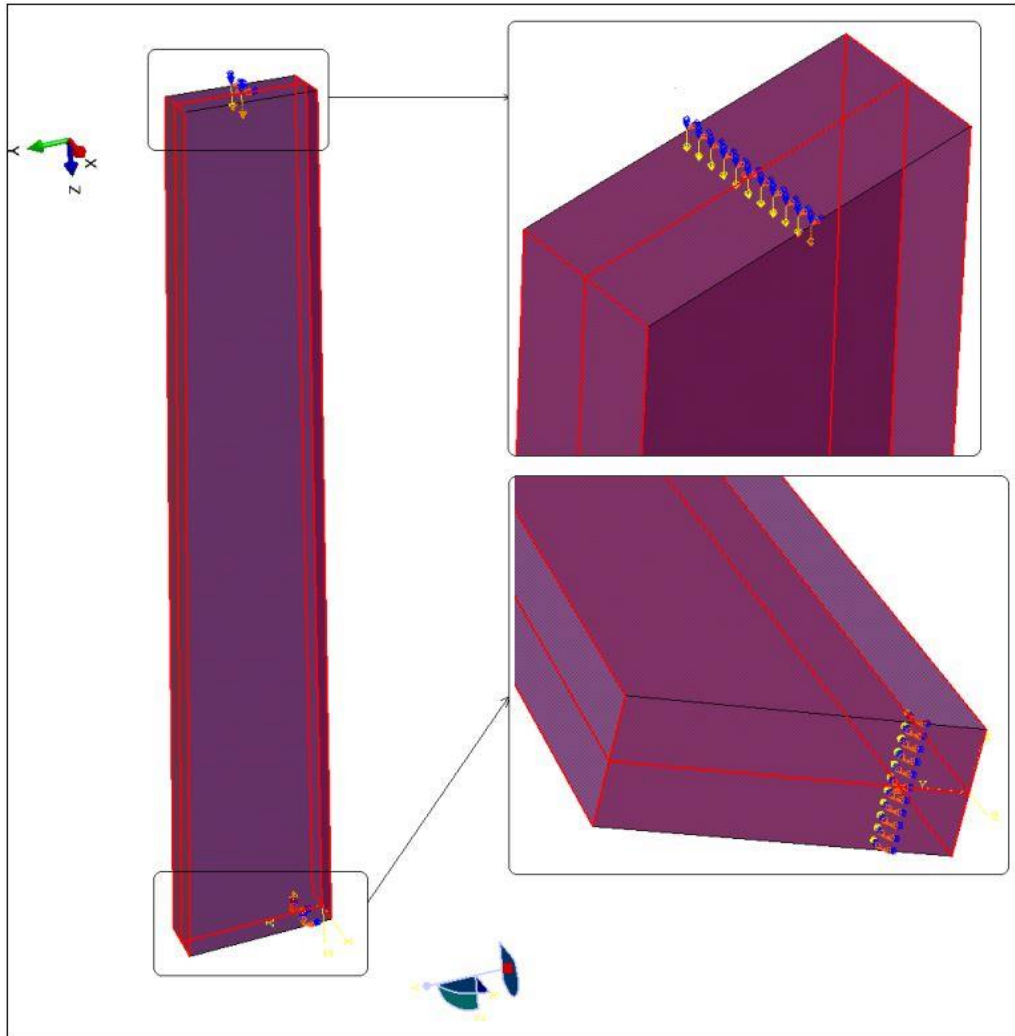


Figure 26: Boundary conditions and illustration of the heated part

On the superior end plate, the load is applied to all the nodes drawing the line of the load application zone, as for the fourth example, see Figure 20.

## 6.2 Definition of the geometry and mesh

In order to avoid any undesirable effects in the load application points, a thickness of 40 mm will be adopted for both end plates.

Following the same assumption as for the first example, only the use of a global imperfection is made. The amplitude is proposed as:  $L/500$ .  $L$  is the distance between both end plates, which is equal to 2.7 m. Thus, the global imperfection is 5.4 mm. Figure 4 illustrates the shape of this global imperfection

For a harmonized numerical simulation, the following mesh size is proposed to all partners. The number of elements in which each side is divided is represented in the figure below:

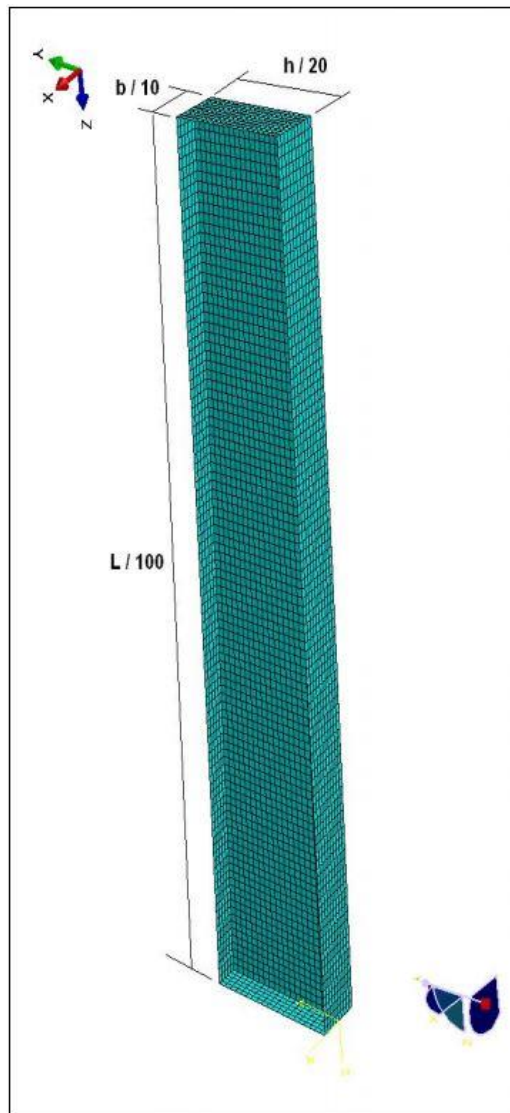


Figure 27: Definition of mesh size

### 6.3 Results

The following tables and figures illustrate the failure load and load horizontal displacement in the strong axis obtained by the partners for the 5<sup>th</sup> example of the benchmark study under the three different computer codes:

FAILURE LOAD (kN) at 500 °C				
CTICM (ANSYS)	CTU (ABAQUS)	TECNALIA (ABAQUS)	UAVR (SAFIR)	ULG (SAFIR)
230.30	235.20	216.15	230.12	227.94

Figure 28: Failure load of column from the 5<sup>th</sup> example

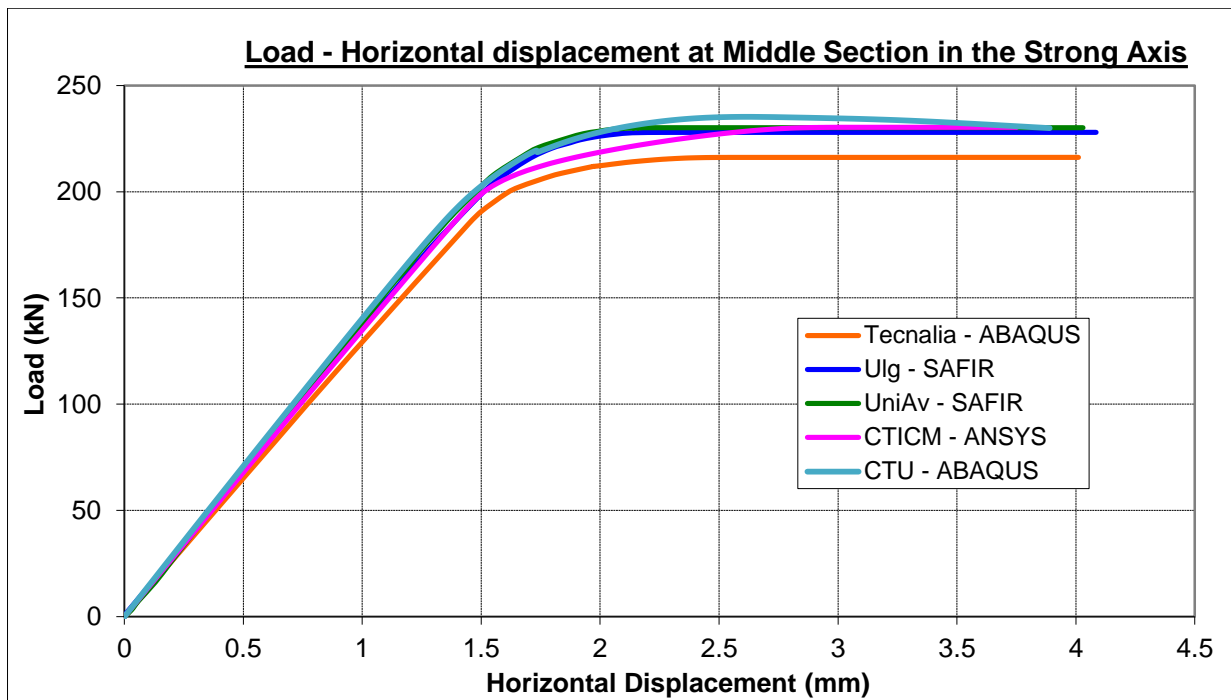
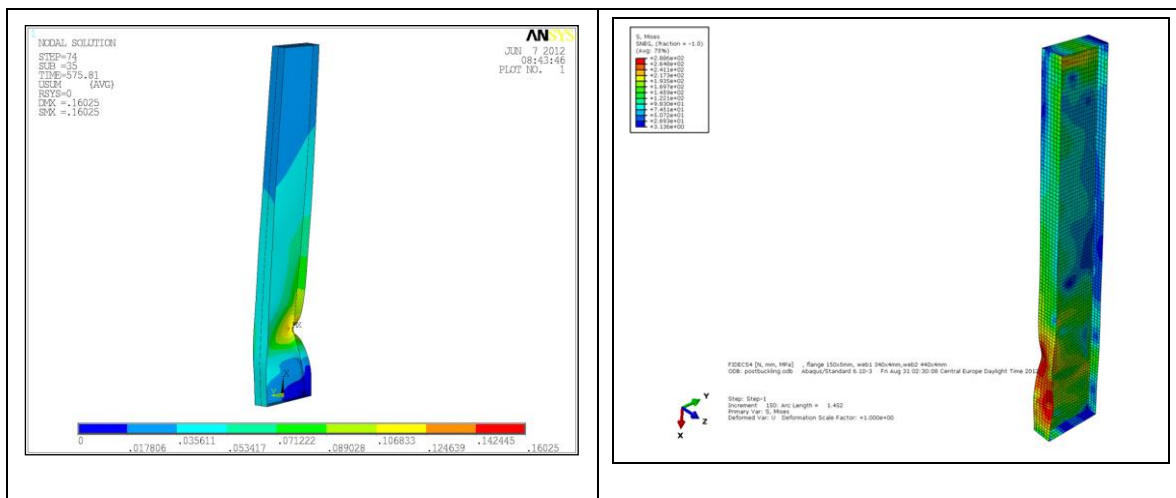
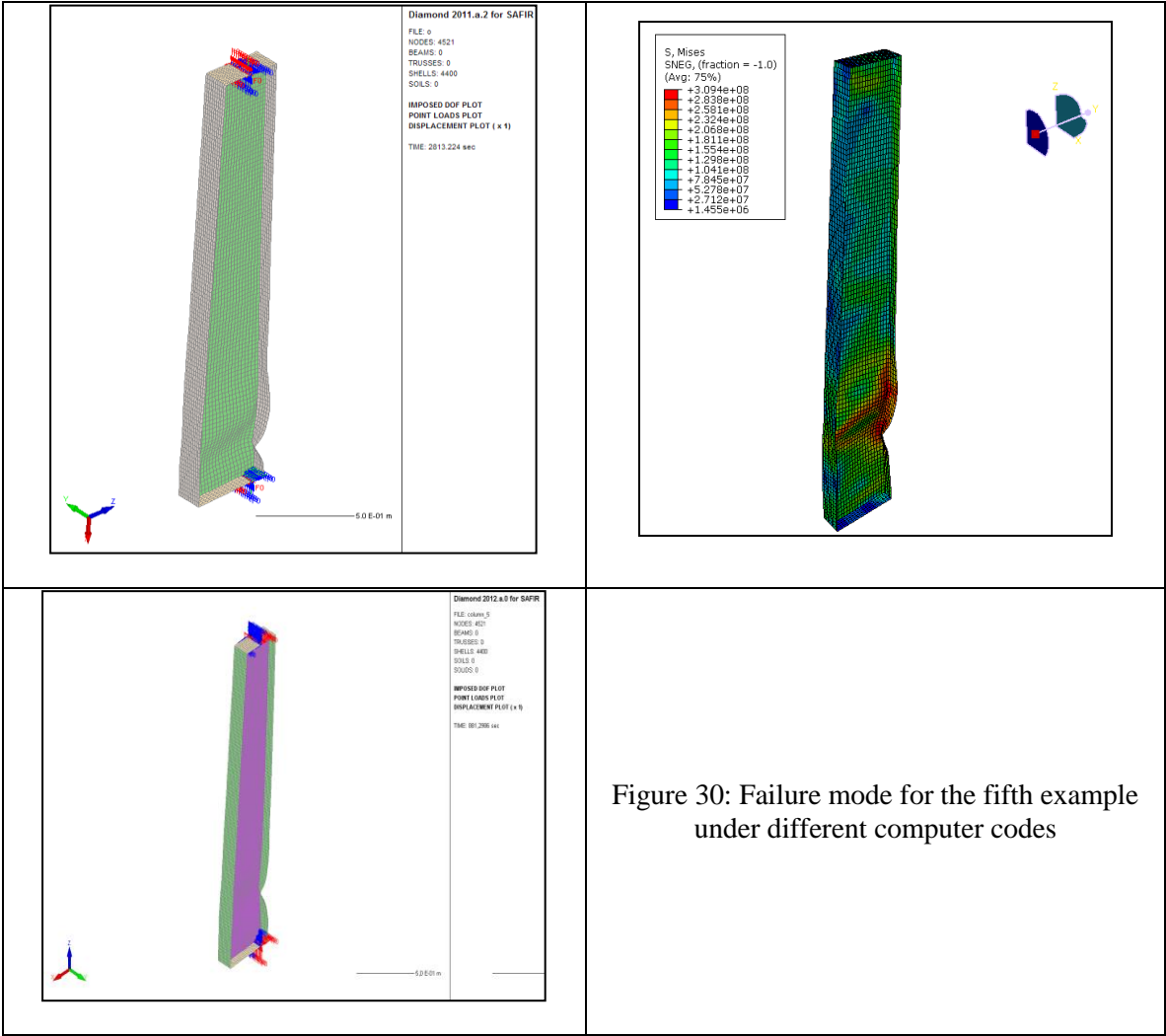


Figure 29: Load – horizontal displacement at middle section in the strong axis for the 5<sup>th</sup> example

The failure modes of the beams of example 5 obtained with the different softwares are shown hereafter:





## 7 6<sup>th</sup> example: single span frame

The single portal frame investigated for the sixth example is shown in the following figure. At both supports, deformations in all directions are prevented. At the nodes where purlins and girts are located, displacements are also restrained in the perpendicular direction of the frame. The entire portal frame is heated up until failure. At the locations of the purlins a load of 3.5 kN is applied on all nodes of the upper flange. Self-weight of the structure is also considered.

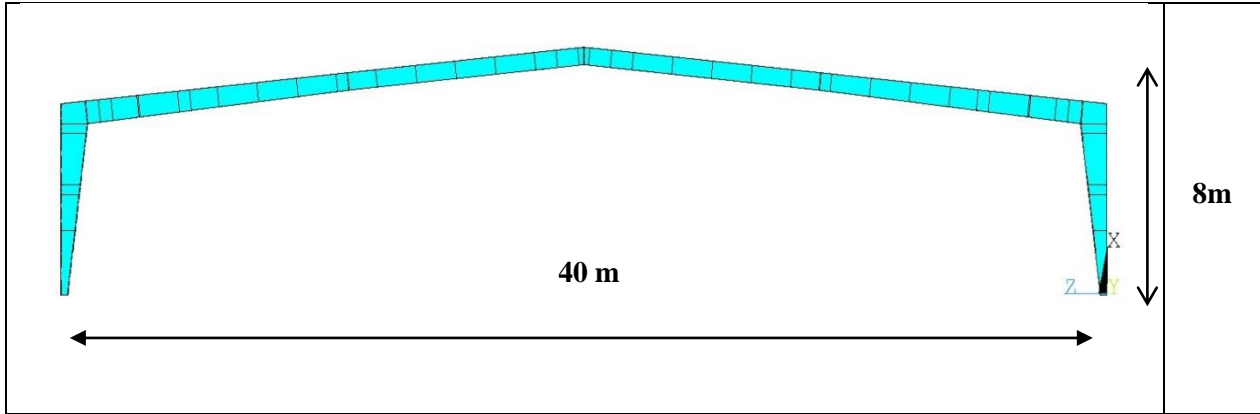


Figure 31: 6<sup>th</sup> example for benchmark study

### 7.1 Definition of load application and boundary conditions

The boundary conditions proposed for the 6th example are represented in the following figure. At both supports, deformation in all directions has been restrained along the line of two nodes. At the nodes where purlins and girts are located, deformation has been restrained in the perpendicular direction to the portal frame. The entire portal frame would be heated up until failure.

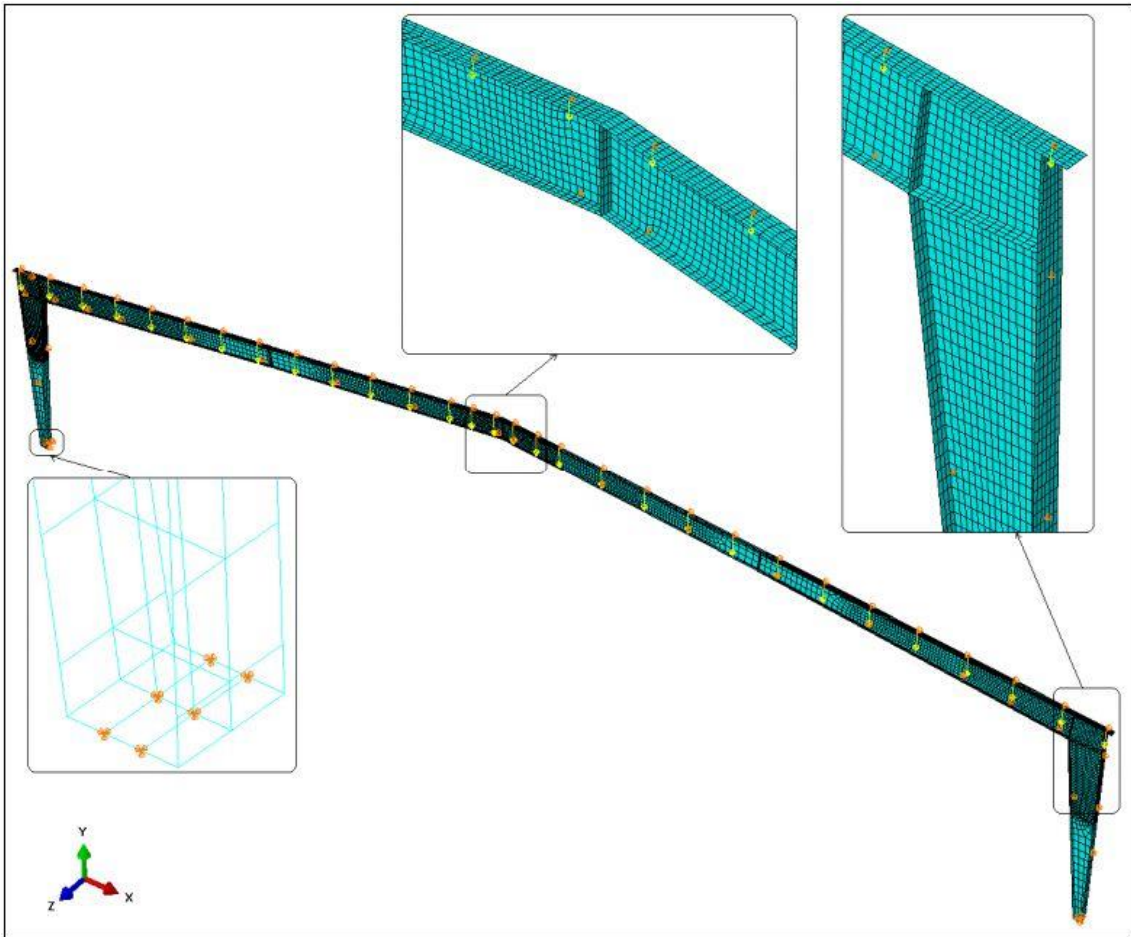


Figure 32: Boundary conditions

On the upper flange of the beams, where the purlins are located, a load of 3.5 kN is applied, see Figure 33. Self-weight of the structure ( $g = 9.8 \text{ m.s}^{-2}$ ) is also taken into account in the simulations:

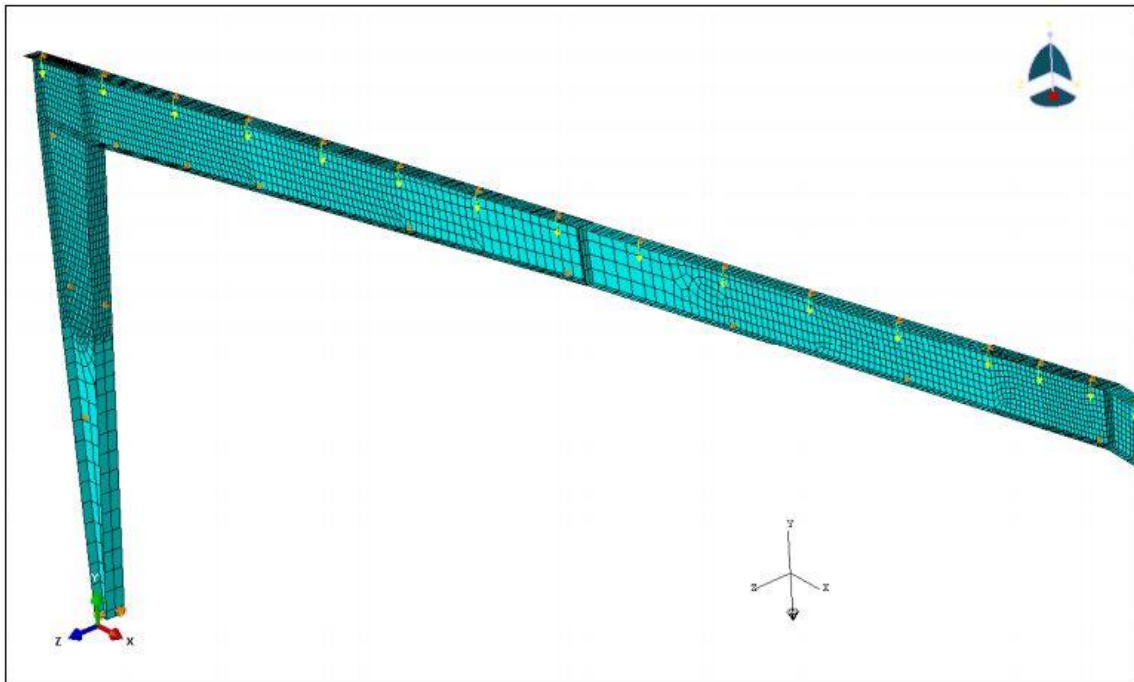


Figure 33: Load application for the numerical simulation

## 7.2 Definition of the geometry and mesh

To avoid any undesirable effects, a thickness of 20 mm is adopted for the supports. For the investigated case, considering that the frame is not sensitive to buckling in a sway mode, the imperfection in form of an initial sway imperfection and the individual bow imperfection of members is not to be taken into account. Therefore, the only imperfection to be added to the frame is a function of the buckling modes obtained in the buckling analysis. Some previous numerical analyses have been performed with the computer code ABAQUS, and the results show small differences when the portal frame is analysed without imperfections and including the imperfections obtained from the elastic modal analysis. For this reason, and with the aim of avoiding input differences among the three computer codes, as the linear buckling analysis is not available in SAFIR, it is proposed to the partners of the modelling group not to include initial imperfections while modelling the portal frame. The mesh size is chosen by different partners as it is considered fine enough to correctly represent the behaviour of the frame.

## 7.3 Results

The following table and figures illustrate the results obtained by the partners using the three different softwares:

FAILURE TEMPERATURE (°C)				
CTICM (ANSYS)	CTU (ABAQUS)	TECNALIA (ABAQUS)	UAVR (SAFIR)	ULG (SAFIR)
577.80	***	569.98	593.70	595.19

Figure 34 : Failure temperature of the single frame

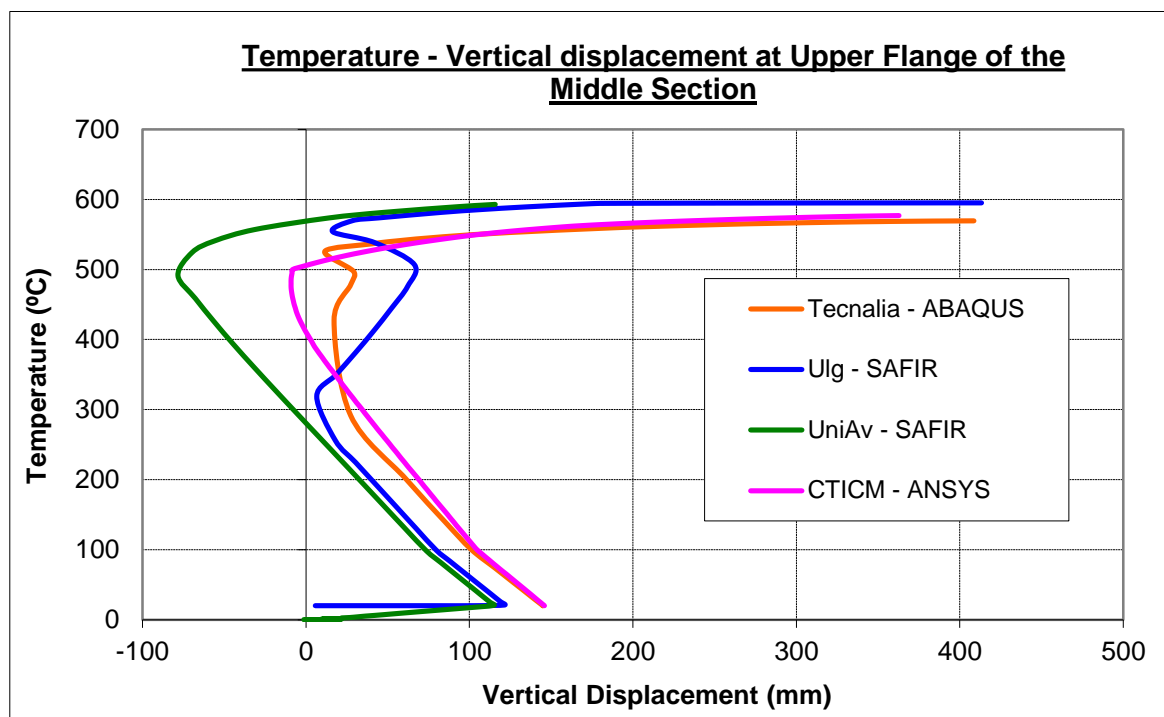
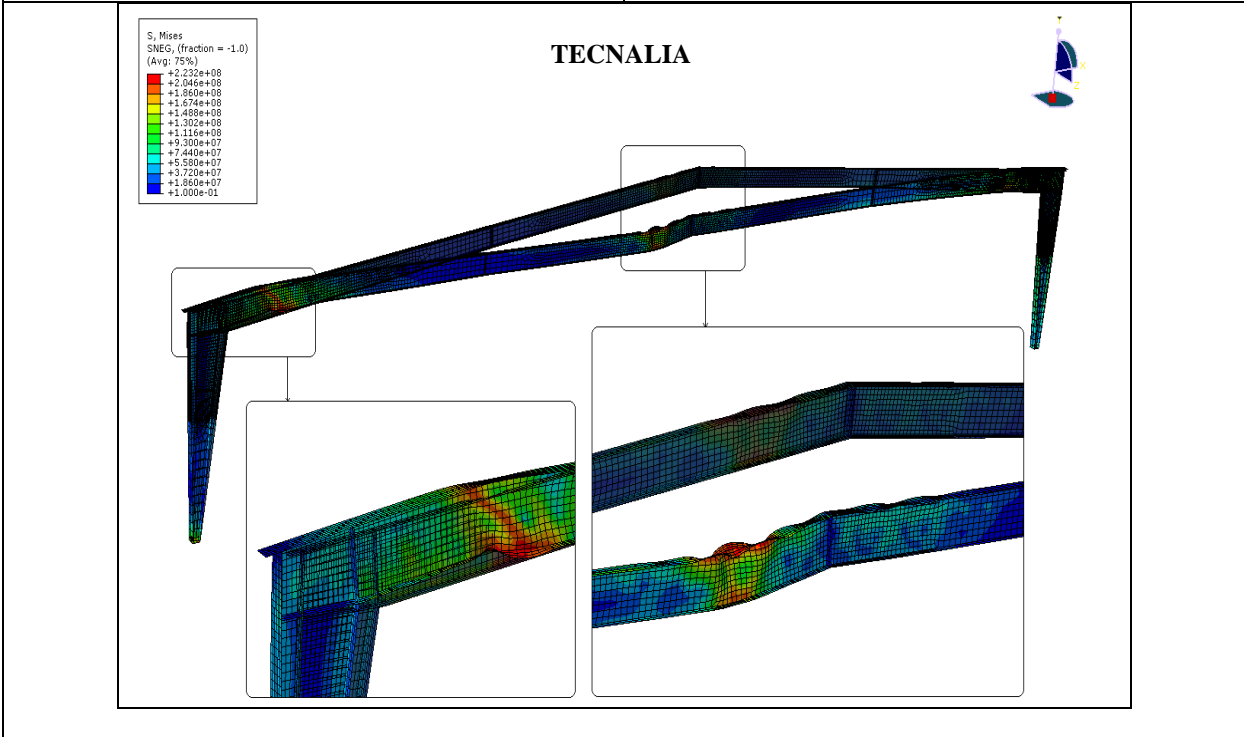
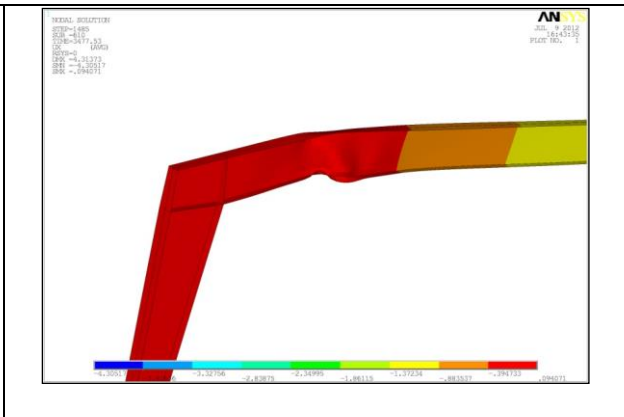
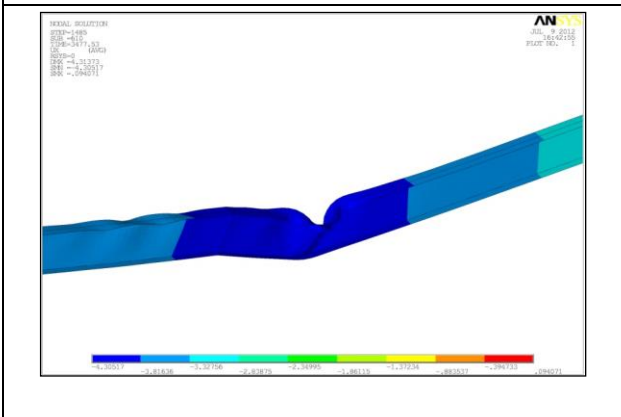
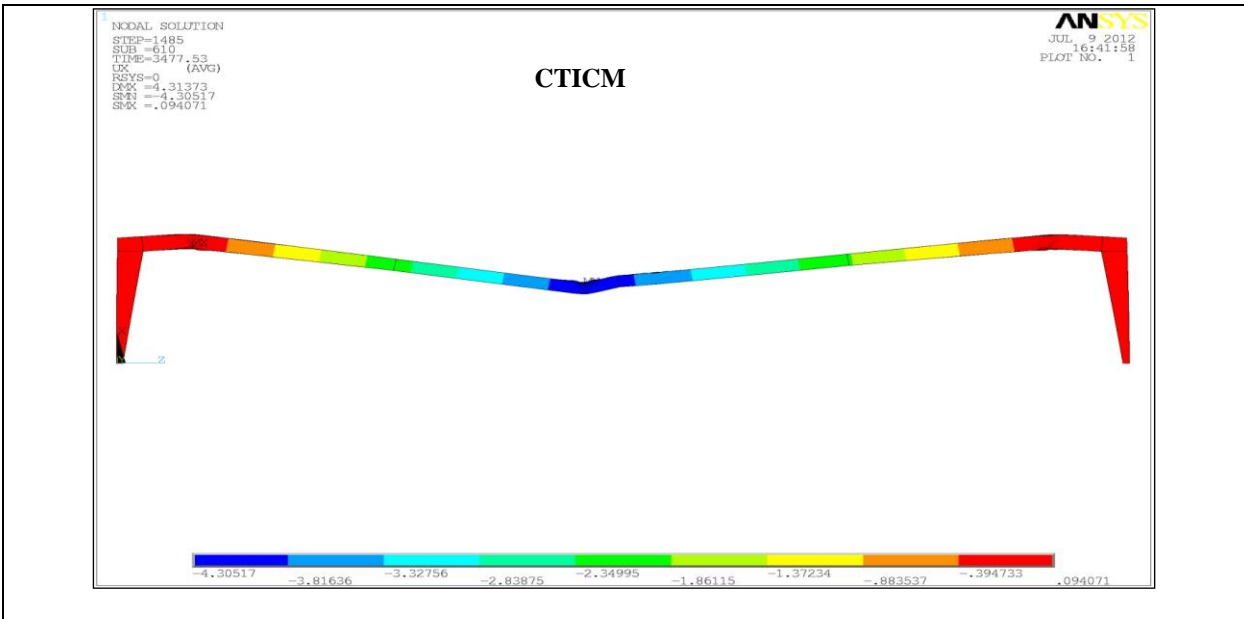


Figure 35: Temperature – vertical displacement at upper flange of the middle section of the frame

The failure mode of the portal frame is illustrated for all softwares in the following pictures:



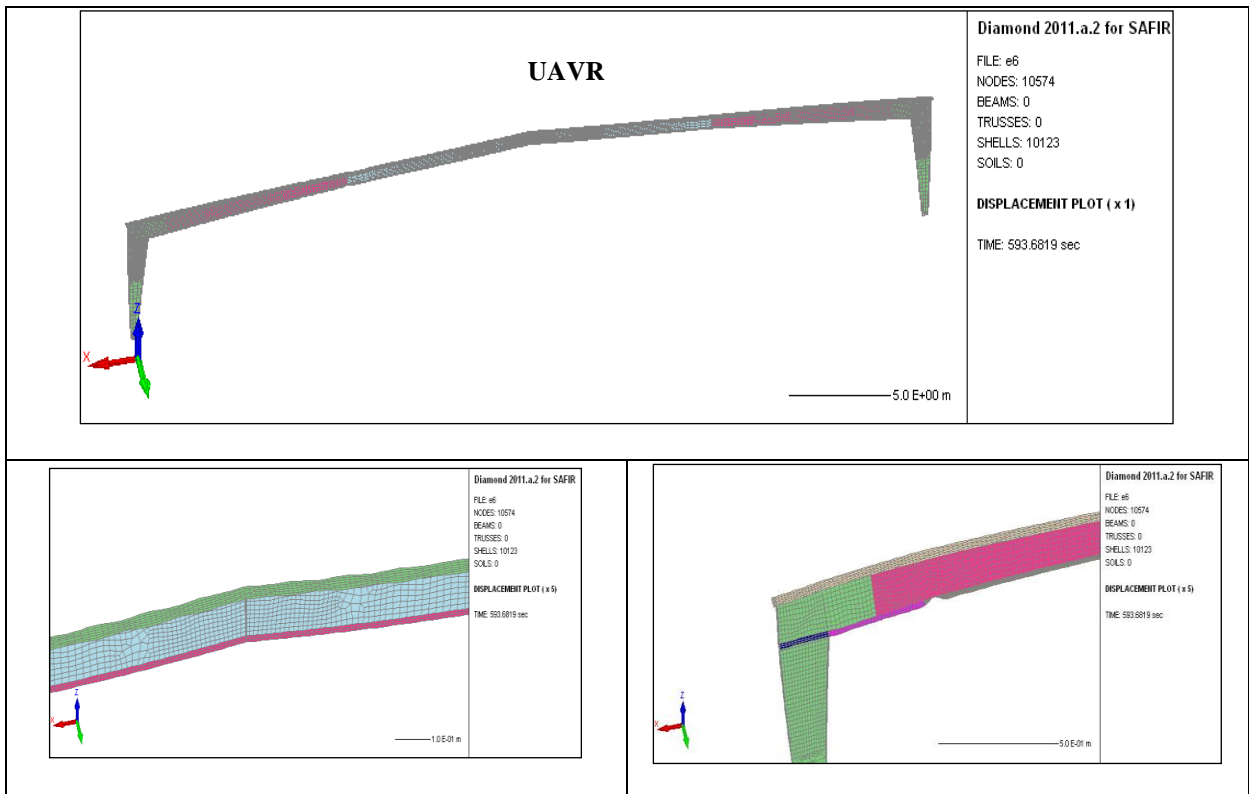


Figure 36: Failure mode of the frame obtained with the different computer codes

## 8 Conclusion

In order to ensure result consistency of the studied computer codes (ABAQUS, ANSYS and SAFIR), a numerical benchmark investigation has been carried out among modelling group of the project. Six different examples have been modelled, five of which will be tested in other Work Packages during the project and a single portal frame. In order to reduce possible input differences among the three computer codes, all the examples have been defined by partners with the same mesh size, initial imperfections, boundary conditions and others to ensure a realistic comparison among all the developed models.

The main results of these simulations have been described in this report and as it can be observed from the results presented in this benchmark study, the models developed with the three different softwares give close results, not only in the studied parameter values, but also in the failure mechanism of the structures.

Regarding Von Mises stresses, in the first stage of the benchmark study, some differences were observed among the stress values provided by all the partners in the defined nodes. Those differences were analysed, looking into the definition of Von Mises stresses in software. It was then noticed that the differences were due to the influence of the computational power of each code, which was able or not to conduct the post-buckling analysis. For that reason, it was agreed to provide the evolution curve of Von Mises stresses for defined elements of each example, which was more appropriate for the comparison of this parameter. With this change, good agreement has been obtained.

Finally, this study showed that assumptions which seemed not to be important at first sight actually were important and must be defined very carefully by engineers in charge of the simulations.